microwave JOURNAL

contents

VOLUME 25, NUMBER 8
USPS 396-250
AUGUST 1982

ON THE COVER: Thomson-CSF's new 3kW TWT covers the new 5.850-6.425 GHz satellite communications uplink band. See the Cover Story on page 114.

Press run for this issue is 44,924 copies.

EXECUTIVE EDITORIAL OFFICE
610 Washington Street, Dedham, MA 02026
Tel: 617 326-8220 710 348-0481
TELEX: 951-659
MICROSOL DEDM

EUROPEAN EDITORIAL OFFICE
25 Victoria Street London SW1H OEH England
Tel: 01-222-0466 **TELEX:** 885744

Microwave Journal is issued without charge upon written request to qualified persons working in that portion of the electronics industry including governmental and university installation that deal with VHF through light frequencies. Other subscriptions; domestic, $36 per year, two year subscriptions $65; foreign, $48 per year, two year subscriptions $85: back issues (if available) and single copies $5.00.

POSTMASTER: send address corrections to Microwave Journal, 610 Washington Street, Dedham MA 02026.

BPA

Horizon House also publishes Telecommunications and Journal of Electronic Defense

Microwave Technology Development Under INTELSAT R&D — a Review

K. Betaharon and P. De Santis
INTELSAT

Introduction

INTELSAT has been active in satellite technologies for more than ten years. Recently a survey paper[1] on the major technological achievements of INTELSAT R&D has been published covering satellite digital communications, intersatellite links, antennas, transponders, and spacecraft technologies. The reader is referred to this paper for a proper perspective of INTELSAT R&D including some aspects of microwave R&D presented here.

The present paper reviews the most recent advances in microwave R&D, both in-house and at a large number of organizations worldwide under INTELSAT sponsorship. Fifteen Development Projects (DP) and five Exploratory Research and Studies (ER&S) are currently in progress within the microwave R&D area. These offer a complete picture of the microwave technologies being developed for future generations of INTELSAT satellites.

In the next four sections we shall illustrate the microwave hardware developed to implement the RF signal functions, such as on-board regeneration, microwave switching, linearization of power amplifiers, and solid-state power amplifiers. In the next two sections, we shall deal with the impact of state-of-the-art technologies, such as GaAs monolithic MIC's and dielectric resonator MIC's, on traditional microwave subsytems. In the last section, practical implementation of the Intersatellite Link microwave subsytems will be described.

On-Board Regeneration

In future satellite communications systems, a higher efficiency will be achieved by sophisticated on-board signal processing techniques involving demodulation of the incoming signal to baseband, subsequent signal routing, and remodulation. This process, in general, is referred to as on-board regeneration.

A number of INTELSAT R&D projects have already contributed toward the development of the hardware technologies necessary to implement on-board regeneration. As early as 1979 a 6 GHz, 120 Mbit/s DQPSK (differential) demodulator with an associated baseband regenerator was developed and delivered successfully by NEC (Japan) under INTELSAT contract IS-894.[2]

More recently, attention has been devoted by INTELSAT to the problems associated with the fabrication of on-board regenerative repeaters compatible with TDMA operation using CQPSK (coherent) demodulation techniques under a contract with MATRA—INTERTECHNIQUE (France). The repeater consists of a CQPSK demodulator followed by a pulse regeneration circuit together with a QPSK modulator (Figure 1) operating at 4 GHz with a 120 Mbit/s rate. Table I summarizes the electrical specifications of the modem. From this table the reader can appreciate that a number of critical RF components, e.g. the spectrum shaping filters and the AFC loop, must be developed for this modem. One of the main goals of this contract is the improvement of present technologies to reduce the mass and power requirements of on-board modems.

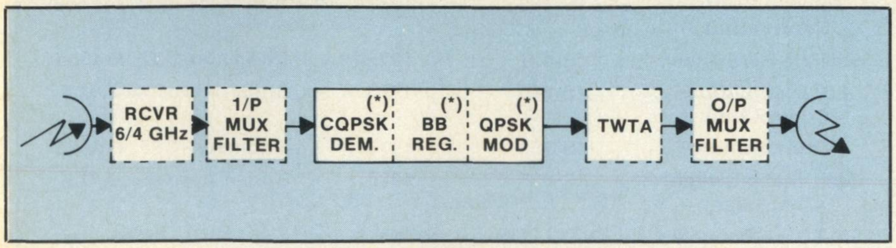

Fig. 1 On-board regenerative repeater
(*) Contract Intel-139 (Matra-Intertechnique, France).

On-Board Switching

In 1986, when INTELSAT VI will be operational, for the first time in the history of INTELSAT a satellite will use on-board dynamic switching to interconnect signals from and to different earth stations. The on-board switching center will operate in the Satellite Switched Time Division Multiple Access (SS—TDMA) mode, and will switch QPSK modulated microwave beams at the uniform rate of 120 Mbit/s.

Many switching elements are needed on-board INTELSAT satellites. They belong to three cate-

[Continued on page 44]

gories: redundancy, static, and dynamic switches. The prime function of each category usually determines the speed, size, power consumption, and as a consequence, the technology of each switch. These categories of switches have been, and are, the subject of R&D activities at INTELSAT.

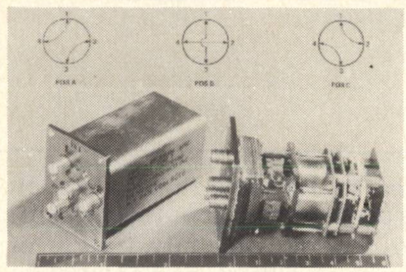

Fig. 2 Engineering model "T" switch (Contract IS-998).

a. **Redundancy Switches** guarantee operation continuity in the presence of failures. They require a very reliable technology in order to operate at any time upon request during the life of the spacecraft.

b. **Static Switches** are, for most cases, in a matrix configuration and are usually formed by a combination of switches listed under (a) above to provide interconnection capability between different receive and transmit beams. They are normally switched in orbit whenever general traffic patterns change and remain unswitched (latched) for long periods of time.

c. **Dynamic Switches** are normally in a matrix configuration and provide continuous interconnection capability between re-

TABLE I

PERFORMANCE OBJECTIVES OF ON-BOARD MICROWAVE MODEM

(Intelsat Contract Intel-139)

DEMODULATOR (CQPSK TYPE)	
I/P level	0 to -15 dBm
Center Frequency	3950 MHz
Carrier Drift Handling Capability	0 to ± 80 kHz Max.
Data rate	120 Mbps
Burst-to-burst	
Frequency difference	0 to 12 kHz max.
Power difference	5dB max.
Clock Stability	$\pm 1 \times 10^{-6}$
MODULATOR (QPSK TYPE)	
Input Signal (data)	Two simultaneous bit streams
Data Rate	60 Mbps/bit stream
Carrier Frequency	3950 MHz
Carrier Stability	1×10^{-7}
Symbol to symbol	
Phase Accuracy	Better than ± 2°
Amplitude Accuracy	± 1 dB max. per symbol

TABLE II

INTELSAT ON-BOARD SWITCH DEVELOPMENT PROJECTS

SUBJECT	CONTRACT NO.	YEAR	CONTRACTOR
Satellite Switch Control Unit	IS-466	1972	Intertechnique, France
Satellite RF Switch	IS-472	1972	Thomson-CSF, France
LSI Distribution Control Unit	IS-563	1973	British Aerospace, U.K.
Matrix Switch	IS-765	1975	Thomson-CSF, France
Semi-Static Switch Controller	IS-835	1976	British Aerospace, U.K.
SS-TDMA Reliable Switch Development	INTEL-119	1981	NEC, Japan

[Continued on page 46]

TABLE III
INTELSAT'S SATELLITE HPA LINEARIZATION DEVELOPMENT PROJECTS

CONTRACT	CONTRACT NO.	YEAR	CONTRACTOR
Butler Matrix	IS-565	1974	ELAB, Norway
Transponder Linearizer	IS-733	1977	Marconi, U.K.
TWTA Linearizer	IS-1001	1978	Thomson-CSF, France
Linearization Mechanisms for Solid State Power Amplifier	INTEL-172	1981	AEG-Telefunken, Germany

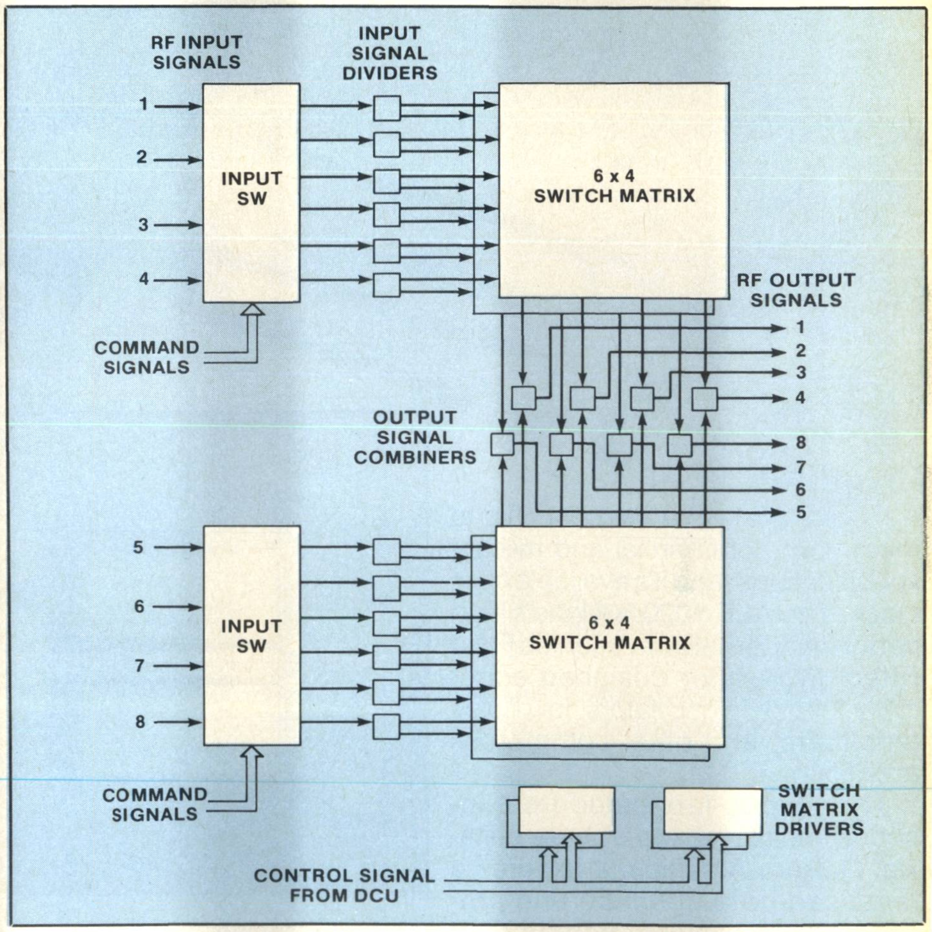

Fig. 3 Block diagram of microwave switch matrix (Intelsat Contract Intel-119).

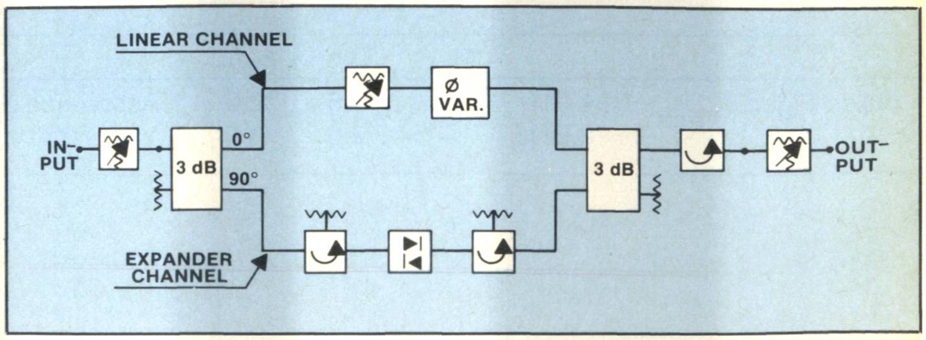

Fig. 4 Thomson-CSF linearizer for TWTA (Intelsat Contract IS-1001).

[*Continued on page 48*]

ceive and transmit beams, usually at high speeds, e.g. in the SS-TDMA mode of operation.

Development of special redundancy switches is the object of Contract IS-998 awarded to Transco Products (USA). The contract calls for the development of coaxial "T" switches operating over the 3.7 - 4.2 GHz band. The latching type switch performance requires 18V, 500 mA pulses of 70 ms duration. The weight of the switch is 110 grams. Figure 2 shows a photograph of the engineering model and sketches of its three possible configurations. This type of switch, or similar ones, may be used for both redundancy switches and/or static switch matrices on-board satellites.[3]

Dynamic switch matrices have been developed in the past by INTELSAT R&D[4] and are being further developed under current contract INTEL-119 (NEC, Japan). Table II refers to INTLESAT's past and present R&D activities in the field of on-board switching matrices. Figure 3 shows the RF block diagram of the 8x8 dynamic microwave switch matrix (MSM). This is a planar MSM in (6x8)x2 configuration with two redundant rows for four working rows. Both the PIN diode and the FET are under examination as switching elements. For the latter, the major MSM RF performance requirements are as follows:

Operational frequency	3950 ± MHz, min.
Insertion loss, in/out	9 dB, max.
Insertion loss variation over the 500 MHz bandwidth, any one path	1.5 dB peak to peak, max. and 0.5 db/MHz max. slope
Insertion loss variation from path to path	2.0 dB peak to peak, max.
RF isolation between any two non-connected ports at any frequency within the 500 MHz bandwidth	50 dB
Switching speed (RF-envelope including all switching transients)	75 ns

TABLE IV

(a) INTELSAT'S 4 GHz SOLID-STATE AMPLIFIER DEVELOPMENT PROJECTS

DEVICE			AMPLIFIER		
Performance Objective	Contractor & Contract No.	Contract End	Performance Objective	Contractor Contract No.	Contract End
5W FET development	MSC IS-906	1981	0.5 W Output Stage	RCA IS-764	1978
6.5W FET development (higher efficiency and more linear than IS-906)	Raytheon INTEL-189	Current	6.5 W SSPA	RCA IS-1000	1981
			6 W and 10 W SSPA qualification	RCA INTEL-138	Current

(b) INTELSAT'S 11 GHz SOLID-STATE AMPLIFIER DEVELOPMENT PROJECTS

DEVICE			AMPLIFIER		
Peformance Objective	Contractor & Contract No.	Contract End	Performance Objective	Contractor Contract No.	Contract End
0.5W FET development	Plessey IS-839	1979	10W TWTA replacement SSPA	RCA INTEL-130	current
5W FET development	Raytheon IS-1007	current			

The above requirements must be met in a unit which is reliable, lightweight, and consumes minimum satellite power. Suitable space qualified technologies must be utilized to achieve the above goals.

On-Board Linearization of Power Amplifiers

On-board power amplifier linearization has a potential impact on future satellite communications. In the last few years various techniques have been explored by INTELSAT to achieve satellite transponder linearization. Table III shows a list of the Development Project contracts relative to on-board linearization awarded in the time period 1974-1982. Here

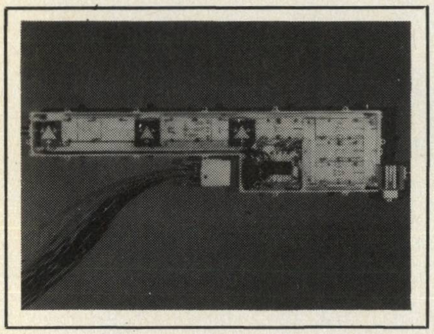

Fig. 5 6 W, 4 GHz solid state power amplifier. (Contract IS - 1000).

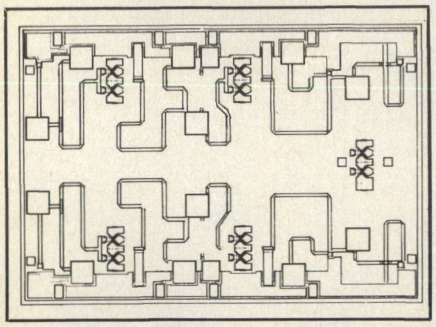

Fig. 6 Front end pre-amplifier for the 6/4 GHz receiver (Contract Intel-143).

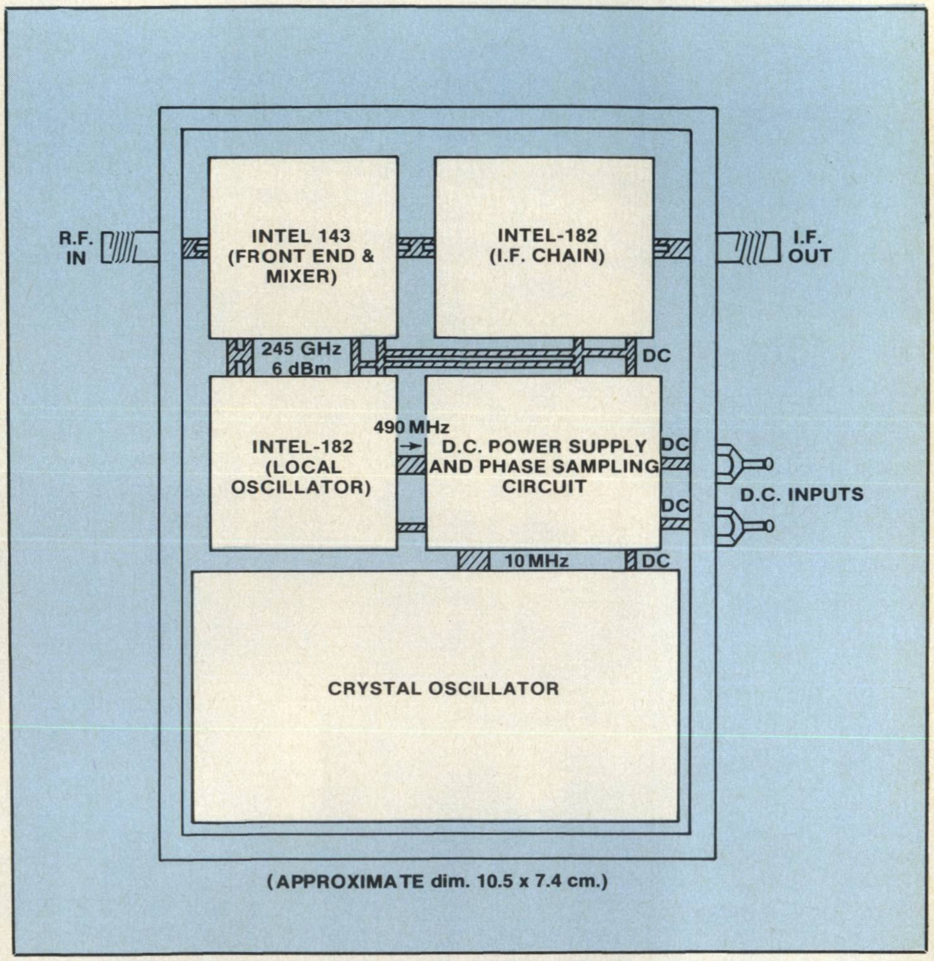

Fig. 7 Integrated 6/4 GHz receiver in test enclosure — plan view (Intelsat Contracts Intel-143 and -182).

[Continued on page 53]

[*From page 49*] **INTELSAT R & D**

we shall report only on the last two contracts: IS-1001 to Thomson-CSF (France) on TWTA linearization, and INTEL-172 to AEG-Telefunken (Germany) on Solid State Power Amplifier (SSPA) linearization.

— TWTA Linearization

A description of the linearizer developed under contract IS-1001 is presented in Reference 5 and a block schematic is shown in Figure 4. The linear branch consists of a variable attenuator and a variable phase-shifter. The non-linear branch uses a pair of back-to-back Schottky diodes.

Although the project has not been entirely completed, preliminary results indicate that substantial improvements in Carrier-to-Intermodulation ratio (C/I) can be realized with this linearizer.

— SSPA Linearization

This more recent contract is intended for linearization of SSPA used as TWTA replacement at 4 GHz. Eventually, it is hoped that it will lead to an all solid state linearized power amplifier. The predistortion linearizer being developed is based on the well experimented technique of using FET amplifiers operated in their linear and non-linear regions. respectively, for the linear and non-linear branches of the linearizing bridge circuit.

Solid State Power Amplifiers

Higher predicted reliability, compared to TWTA's, and the recent rapid progress of FET devices have made SSPA's suitable for microwave power amplifiers. INTELSAT started an effort of solid state power amplifier development as early as 1977. This effort has concentrated on both device and amplifier development for the presently utilized satellite transmit bands (4 and 11 GHz). Table IV shows each contract effort with its objectives. Figure 5 shows a photograph of the most recently completed contract, the 6 W, 4 GHz TWTA replacement SSPA.[6] The amplifier has a bandwidth of 500 MHz, with a small signal gain of 56 dB and an efficiency of around 15% (at saturation). A similar 10 W amplifier will be flight-qualified under a separate current contract.

[*Continued on page 54*]

[*From page 53*] **INTELSAT R & D**

GaAs Monolithic Circuits

Monolithic Microwave Integrated Circuit (MMIC) technologies are being developed for an increasing number of analog and digital applications. Most of the typical MMIC features seem very attractive for space applications. More specifically, the four most distinct GaAs MMIC features relevant to satellite applications are:

- small size and weight
- low dc power consumption
- good radiation hardening characteristics, and
- capability to combine analog and digital signal processing on same chip.

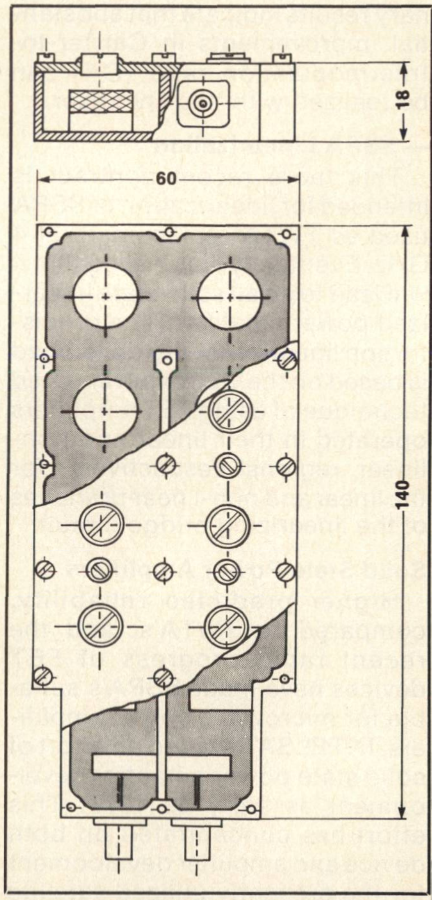

Fig. 8 4 GHZ .9% BW channel filter physical layout (Intelsat Contract Intel-183).

The purpose of INTELSAT R&D in this field is to assess how the above MMIC properties can be usefully exploited on-board future satellites. To this end, two development projects have been undertaken to build a monolithic satellite receiver.

Under contract INTEL-143, "Wideband Integrated Receiver Development," an MMIC pre-am-

[*Continued on page 56*]

[From page 54] INTELSAT R & D

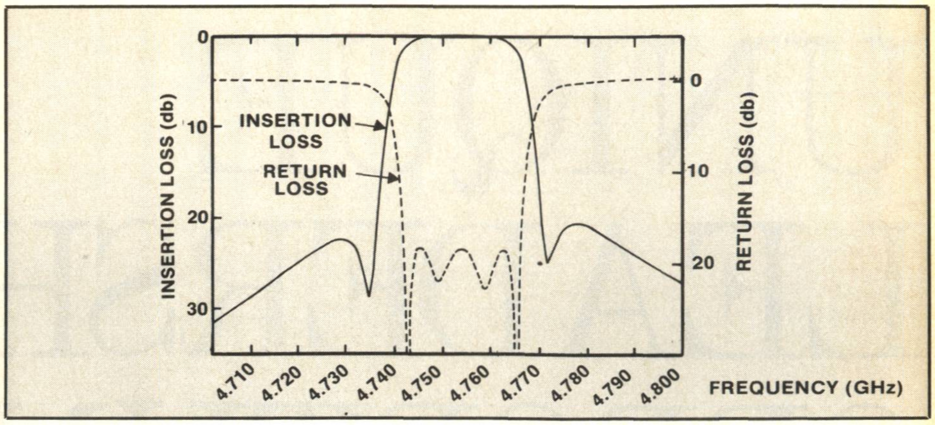

Fig. 9 Measured insertion and return loss response of 4-pole dielectric resonator filter (Intelsat ER & S project).

TABLE V
INTERSATELLITE LINK SUBSYSTEM DEVELOPMENT PROJECTS

ITEM	PERFORMANCE OBJECTIVES	CONTRCTR	PROJECT NUMBER	REMARKS	CONTRACT END
TWT(A)	10 Watts Output 23 & 33 GHz 37% Efficiency 43-49 dB Gain	Hughes-EDD (U.S.)	78 101	Breadboard Models & Engineering Models	Mid '82 End '82
Wideband FM Modem	23 GHz 1% Linearity 10-130 MHz Baseband Stability: 1×10^{-4}	GE (U.S.)	59	Breadboard Model Only	Early '82
Frequency Converters (item i through iv include IF amplifiers)	(i) 4 GHz/70 MHz; 7 dB NF 20-25 dB gain (ii) 70 MHz/4 GHz; 10 dB NF 25-30 dB Gain (iii) 23 GHz/6 GHz; 7 dB NF 20-25 dB Gain (iv) 33 GHz/6 GHz; 7 dB NF 20 dB Gain	NEC (Japan)	103	Breadboard models & Engineering models	End '82
	(v) 4 GHz/23 GHz; 5 dB NF, 4 dB Conv. Loss (vi) 4 GHz/33 GHz; 5.5 dB NF 4.5 dB Conv. Loss	NEC (Japan)	151	Breadboard Models & Engineering Models	Mid '83
Low Noise Amplifier	23 GHz; 4.8 dB NF 20 dB Gain 1 GHz Bandwidth	NEC (Japan)	104	Breadboard Model & Engineering Model	Mid '82
ISL Test Bed	Capabilities to Simulate Various System Configurations	COMSAT Labs (U.S.)	LAC		End '83
Low Noise Receiver	33 GHz (4 GHz IF) 20 dB Gain min. 5 dB NF max.	Not awarded yet	167	RFP issued in May	End '83
Low Noise FET Development	2-3 dB NF, 7-10 Gain, at 23 GHz 3-4 dB NF, 4-6 Gain, at 33 GHz 1 GHz Bandwidth for both units	Plessey (U.K.)	142		End '83

[Continued on page 58]

[*From page 56*] **INTELSAT R & D**

plifier mixer front-end for a 6/4 GHz receiver is being built. Figure 6 shows the RF pre-amplifier circuit as developed by Plessey (U.K.) operating over the frequency band 5.85 - 7.075 GHz. The overall front-end gain is 20 dB with a noise figure of 3 dB.

Under contract INTEL-182, "Monolithic Wideband 6/4 GHz Receiver Development," a Local Oscillator (LO) and an IF pre-amplifier are being built. They will be subsequently combined with the hardware being developed under the previous contract in order to build a complete monolithic receiver. The LO will be implemented using a SAW delay line. Figure 7 shows the final layout of the monolithic receiver.

Dielectric Resonator Filters

In comparison with waveguide filters, dielectric resonator filters (DRF) present very attractive features of low volume and weight. These properties are particularly important for on-board multiplexers.

Presently, under contract INTEL-183, Elektronikcentralen (Denmark) is developing DRF's with no external group delay equalization, suitable for use on-board future INTELSAT spacecrafts. These are eight pole Chebyschev filters which permit coupling of non-adjacent resonators for internal group delay compensation, and include spurious mode suppression circuits. Figure 8 shows the physical lay-out of a narrowband (0.9% fractional bandwidth) filter operating at 4 GHz.

In addition, under initial Exploratory Research and Studies (ER&S) efforts performed by COMSAT Labs (USA) for INTELSAT, a theoretical investigation of the dielectric resonator oscillator was performed[7] and sample dielectric filters designed, built, and tested. Figure 9 shows a measured frequency response of a 4-pole DRF using the MIC transmission line coupling shown in Figure 10.

Intersatellite Link (ISL)

Under INTELSAT R&D Intersatellite Links (ISL) have been the subject of commendable activity for the past several years. The reader is referred to reference 8

[*Continued on page 60*]

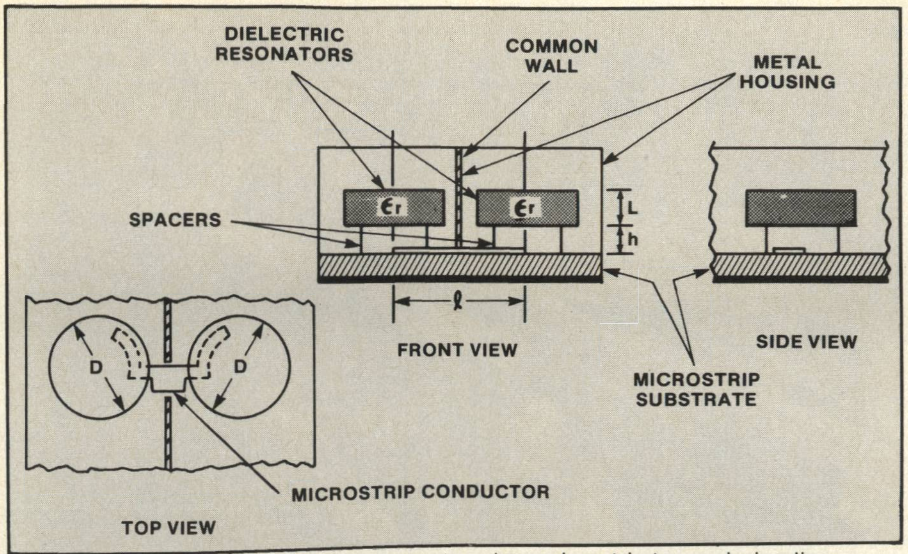

Fig. 10 Coupled dielectric resonators, by a microstrip transmission line (Intelsat ER & S Project).

for an overview of the INTELSAT R&D program related to ISL.

Here we shall limit ourselves to a report on the most recent results achieved by INTELSAT R&D in the hardware implementation of the ISL microwave components. These components refer to the two ISL baseline solutions shown in Figure 11, namely the FM remodulation and the heterodyne repeater ISL. Table V shows the development projects presently underway which relate to ISL RF hardware. A brief description of some of these components is given below.

Wideband FM Modem - Contract INTEL-040, General Electric, USA

Reference 9 provides a full des-

TABLE VI
PERFORMANCE OBJECTIVES OF INTERSATELLITE LINK MODEM
(Contract Intel-059)

MODULATOR		DEMODULATOR	
Output Frequency	23.05 GHz	Input Frequency	6.75 GHz
Output Power	—10 dBm	Input Power	—15 dBm typical
FM Output Bandwidth	1.0 GHz	FM Bandwidth	1 GHz
Input Modulation Frequency	10 to 130 MHz	Deviation Sensitivity	1.0 mV/MHz
Deviation Sensitivity	200 MHz/V	Linearity	better than ± 2%
Linearity	better than ± 2%	Baseband Output Frequency	10 to 130 MHz

[*Continued on page 62*]

cription of the modem developed under this contract. The FM modulator is an FET VCO wherein a 10-130 MHz signal (equivalent to three transponder channels) modulates a 7.8 GHz carrier. A times-three multiplier then produces a 23 GHz signal with a 1 GHz spectral bandwidth. After the down conversion to 6.75 GHz, this signal is frequency demodulated to the 10-130 MHz original bandwidth. The specifications of the modem are shown in Table VI. This project will be completed in 1982. Preliminary results indicate a performance close to the required specifications.

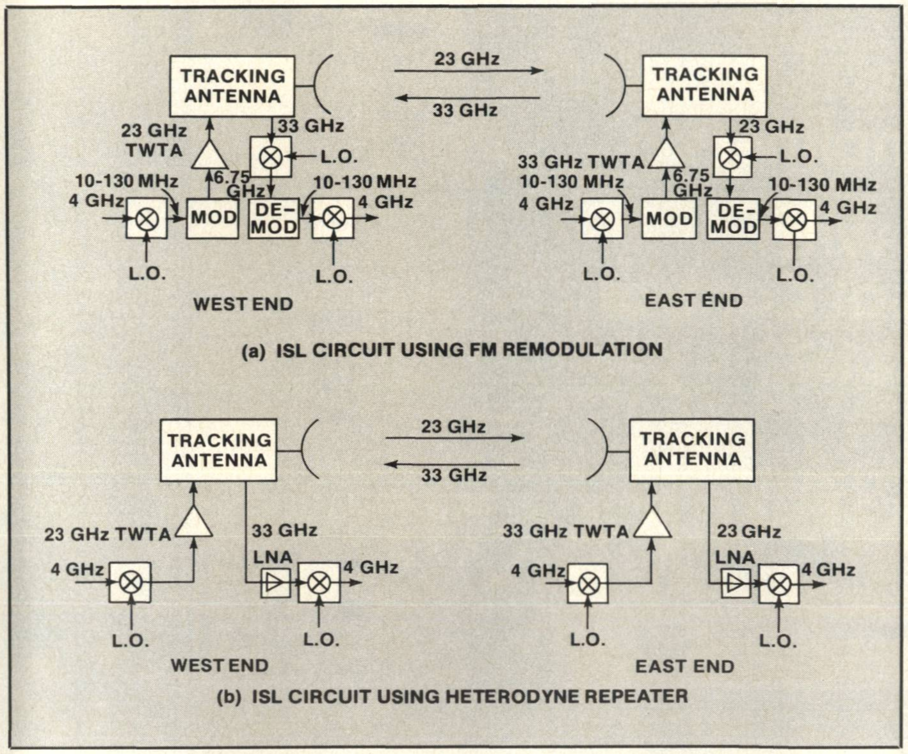

Fig. 11 Intersatellite link baseline systems.

Frequency Converters - Contract INTEL-055, NEC, Japan

The ISL converters cover a wide range of frequencies. Initially, INTELSAT's contract with NEC (Japan) for ISL converters included those four needed for the RF remodulation scheme shown in Figure 11 (a). All four converters include IF pre-amplifiers and all of the RF circuitry are realized in MIC. Reference 10 describes these converters in detail. A photograph of the 23 GHz/6.75 GHz converter/IF pre-amplifier breadboard model is shown in Figure 12. A later contract, also with NEC, calls for development of two upconverters for use in the ISL Heterodyne Repeater scheme.

[*Continued on page 66*]

23 GHz Low-Noise Amplifier - Contract INTEL-056, NEC, Japan

This amplifier is intended for the ISL receiver front-end of the 23 GHz Link. The breadboard model has already been developed and delivered by NEC under contract INTEL056. It meet or exceeds all the requirements of the contract. This amplifer consists of two MIC modules with each module incorporating two low noise FET devices. The two modules are cascaded with an MIC isolator as an intermediate stage. The access to the input and output of the amplifier is through waveguides isolators and waveguide to coaxial transistions. This assures an input/output VSWR match of better than 1.15:1. The total amplifier power (including a dc/dc converter) from 15 V supply is 1 W and this integrated unit weighs 244 grams. Detailed description and measured performance of this amplifier are presented in reference 11. Figure 13 shows a photograph of the 23 GHz amplifier module and the assembled amplifier.

Additional Contracts

Additional contracts, current and forthcoming, are intended for development of the 20 and 30 GHz, low-noise FET devices, as well as the 30 GHz receiver. See Development Projects 167 and 142 in Table 8.1.

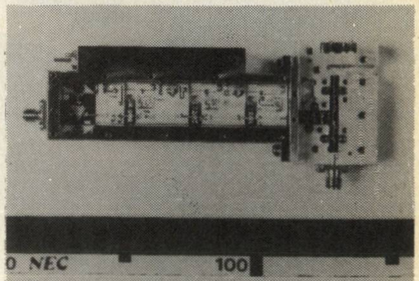

Fig. 12 23 GHz converter/IF amplifier for ISL (Contract Intel - 055).

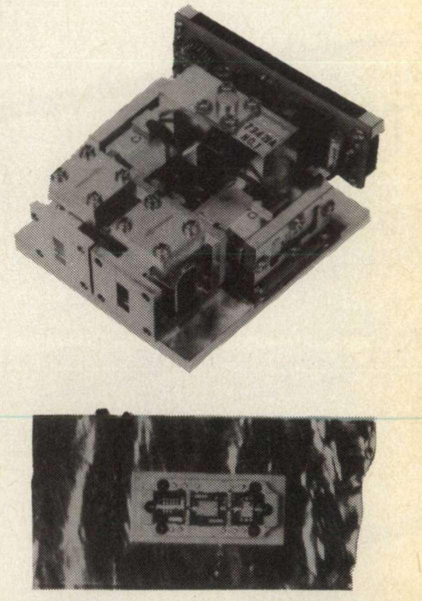

Fig. 13 (a) 23 GHz integrated low noise amplifier for ISL, (b) One module with the cap removed (Contract Intel - 056).

Conclusions

We have presented a review of the most recent advances in microwave technologies achieved through INTELSAT R&D programs. The microwave hardware necessary to implement on-board regeneration, switching and amplifier linearization have been de-

[Continued on page 68]

scribed. Monolithic Microwave Integrated Circuit (MMIC) and dielectric resonator technologies have been shown to play a potentially relevant role in the future INTELSAT spacecraft. The microwave hardware for Intersatellite Links (ISL) has been reported to be in a final state of advancement.

From the above description we can recognize that INTELSAT microwave R&D is motivated by the needs of the future generations of INTELSAT spacecraft and is limited to those areas where particular impetus is deemed necessary to trigger future industrial activity. To avoid duplication of effort, communications satellite related areas of research and development which possess definite application to INTELSAT satellites, but are investigated by the industry, either in the U.S. or abroad, as routine work or as contracts to other interested parties, are not usually pursued by INTELSAT.

Major thrusts for near and medium term microwave R&D will be an increase in hardware reliability, and reduction of weight, volume and dc power consumption. To this end, INTELSAT R&D is already moving in the direction of high density integrated circuits performing both analog and digital functions, e.g. GaAs monolithic switching modules for Microwave Switch Matrices, as well as integrated circuits operating both at RF and baseband frequencies, e.g. composite structures with modems and Baseband Switch Matrices.

REFERENCES

1. Sachdev, K. K., "Satellite Communication Technology Challenges for the 80's", Journal of Spacecraft and Rockets, Vol. 18, No. 2, March-April 1981, pp. 110-118.
2. Shimamura, T., I. Eguchi, F. Assal, "120 Mbit/s, 6 GHz On-Board Waveform Regenerator for Communications", Proceedings of 9th European Microwave Conference, Brighton, England, Sept. 17-20, 1979, pp. 213-217.
3. Assa, F., C. Mahle, and A. Berman, "Network Toplogie to Enhance the Reliability of Communications Satellites", Comsat Technical Review, Vo. 6, No. 2, Fall 1976.
4. Assal, F., and X. Rozec, "Fast, Fully-Redundant, 4 GHz, 8x8 Microwave Switch Matrix for Communications Satellites", 9th European Microwave Conference, Brighton, England, Sept. 17-20, 1979, pp. 218-222.
5. Bremenson, C., et al., "Linearizing TWTA Amplifier in Satellite Transponders - System Aspects and Practical Implementation", AIAA 8th Communications Satellite Systems Conference, Orlando, Florida, April 20-24, 1980, pp. 80-89.
6. Huang, H., B. Dornan, F. Drago and J. Hawley, "C-band FET Power Amplifier for TWTA Replacement", RCA Engineer, Vol. 25, No. 2, Aug./Sept. 1979, pp. 79-82.
7. Bonetti, R., and A. Atia, "Analysis of Microstrip Circuits Coupled to Dielectric Resonators", IEEE Transaction on Microwave Theory and Techniques, Vol. MTT-29, No. 12, Dec. 1981, pp. 1333-1337.
8. Sachdev, D. K., and T. Chidambaram, "Intersatellite Links for International Communications," 1981 IEEE International Conference on Communications, Conference Record, Denver, Colorado, JUne 14-18, 1981, pp. 70.2.1-70.2.6.
9. Prather, W. H., "Development of a Wideband FM Modem For ISL Applications", 1981 IEEE, International Conference on Communications, Conference Record, Denver, Colorado, June 14-15, 1981, pp. 70.4.1-70.4.5.
10. Ogawa, K. Takahashi, H. Ishihara, S. Kitazume, "Mixers and Amplifier for Intersatellite Link Transponders", to be presented at 33rd IAF Congress, Sept./Oct. 1982, Paris, France.
11. Aramake, S. et al, "23 GHz Low Noise Amplifier", to be published in the Symposium of the Institute of Electronics and Communications Engineers of Japan, October 18, 1982. ■

Digital Radio for 90-Mb/s, 16-QAM Transmission at 6 and 11 GHz

J. J. Kenney
Bell Laboratories
North Andover, MA

Introduction

A digital radio system, DR 6-30, has been developed to provide 90-Mb/s capacity (equivalent to 1344 voice channels) in a 30-MHz channel within the 6-GHz common carrier band.[1,2] A companion radio repeater, DR-11-40, extends this capability to the 11-GHz band. Sixteen state quadrature amplitude modulation (16-QAM) is used to obtain a spectral efficiency of 3 bits per hertz, while at the same time causing negligible interference to adjacent digital or analog RF channels.[3] Full route development of 8 RF channels at 6 GHz or 11 RF channels at 11 GHz is possible. This paper first describes the baseband and modem equipment and then focuses on the radio repeater design considerations and hardware realization.

Baseband and Modem Equipment

The DR 6-30/DR 11-40 Digital Radio System has three major functional units: a 90A Line Terminating System, a 90A Regenator Bay, and an IF/RF Radio Bay (either DR 6-30 or DR 11-40). These arrangements are shown in Figure 1. All signal interconnections between these units are at an intermediate frequency of 70 MHz.

The 90A Line Terminating System contains digital terminals, line protection switching, and digital multiplex. A digital terminal transmitter receives two asynchronous unipolar DS-3 rate (44.736 Mb/s) bit streams, synchronizes them, adds overhead bits and produces a 16-QAM modulated IF carrier at 70 MHz.[4] A digital terminal receiver performs the corresponding inverse functions with circuitry somewhat more complex because of the need to recover carrier, timing and framing information from the received signal. Radio protection switching (1xN frequency diversity) is also part of the 90A Line Terminating System. Each received unipolar DS-3 rate signal is monitored for frame integrity and DS-3 parity violations. Transfer of service to the protection channel occurs when frame is lost or when the bit error rate (BER) exceeds a preset threshold of 10^{-6}.

At a repeater station, the transmitted signal is regenerated to preserve maximum immunity to accumulated noise and other distortions. In the regenerator, radio line parity is checked and corrected, parity and misframe indi-

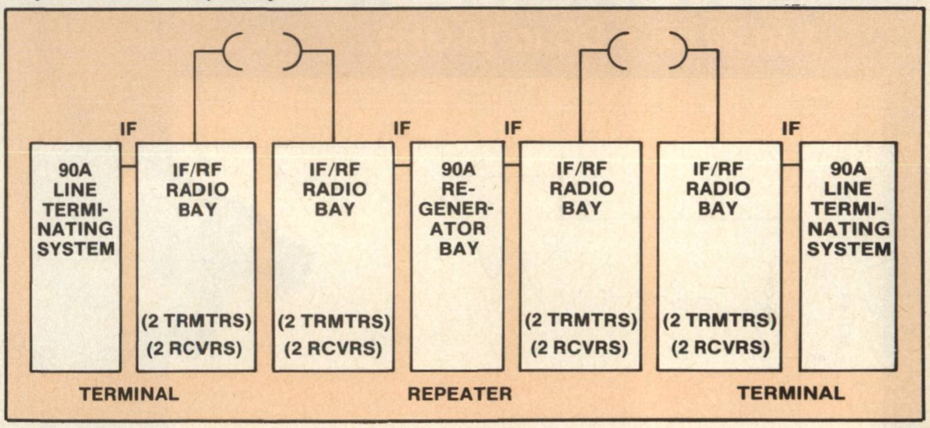

Fig. 1 Typical digital radio system arrangement.

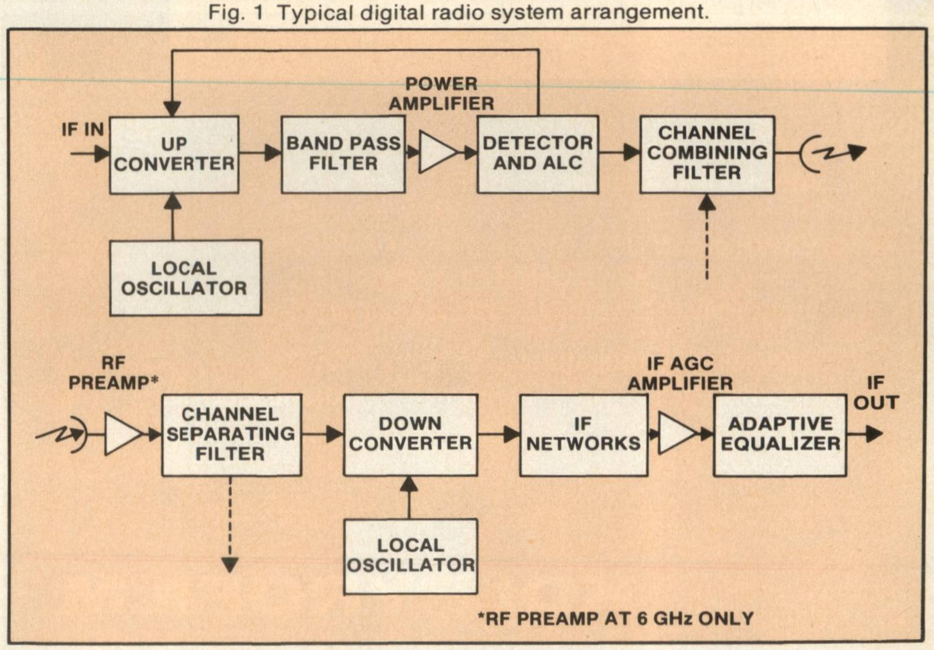

Fig. 2 Transmitter and receiver block diagram.

cations are generated, and service channel bits are extracted and inserted.

Radio Bay

The basic DR 6-30 or DR 11-40 radio bay interconnects with the modem equipment at an IF of 70 MHz (block diagram shown in Figure 2) Conventional heterodyne repeater practices are followed in most respects. The 6- and 11-GHz repeaters are functionally similar but there are significant differences in the implementations of the designs. The radio bays shown in Figure 3, contain two transmitters and two receivers in a 7-foot frame that is 10-1/4 inches square. Few adjustments are required, and access is completely from the front.

Characteristics of the Radio Channel

The digital channel shape is essentially determined by the baseband filtering contained in

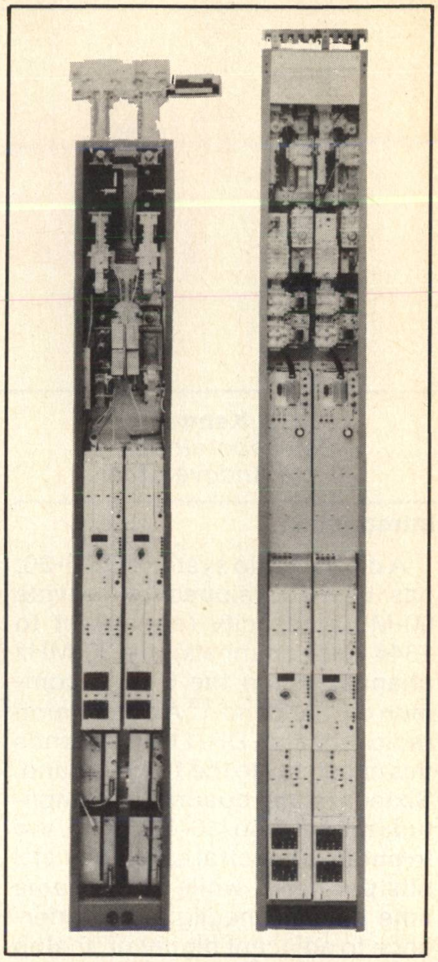

Fig. 3 DR 6-30 (Left) and DR 11-40 (Right) radio bays - two transmitters and two receivers each.

the terminals and regenerators. Thus, the purpose of the radio equipment is to provide a linear channel with minimal dispersion over a 30-MHz bandwidth. The 6- and 11-GHz transmitter-receivers have been designed to provide nearly identical transmission channels, and the two types may be mixed within a common system.

Linear delay distortion may be corrected to within ±1 ns over ±12 MHz at installation by the selection of an appropriate equalizer, and the parabolic delay distortion is equalized to within 1 ns over ±12 MHz. One dB of the accomodation range of the adaptive slope equalizer is allocated to correct asymmetric amplitude shapes. The symmetric component of amplitude shape is equalized to within 1 dB over ±12 MHz.

Amplitude linearity is the principal additional requirement imposed on circuits carrying QAM signals. Linearity budgets have

[Continued on page 74]

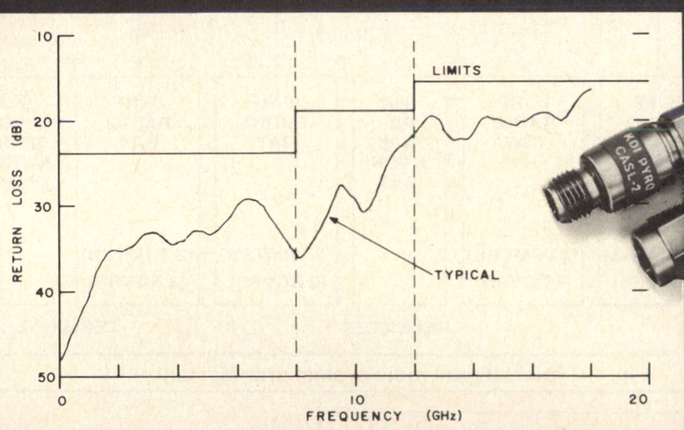

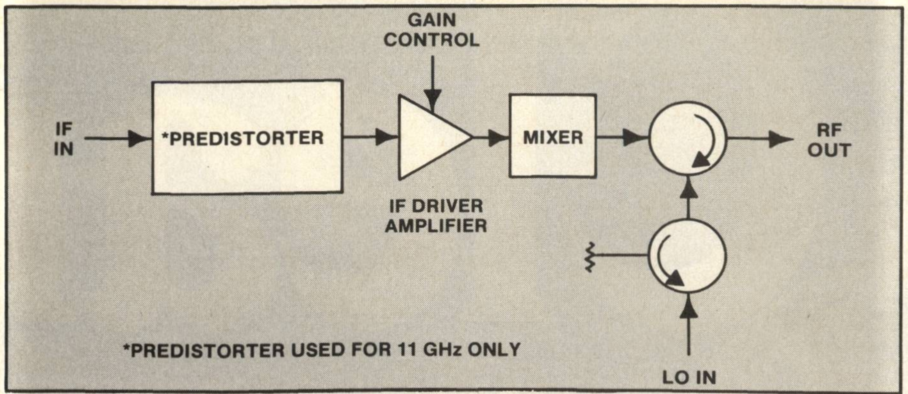

Fig. 4 Upconverter block diagram.

been set up for these few systems by treating the third-order inband intermodulation spectrum as co-channel interference.[2] The transmitter, in particular the RF power amplifier, is the prime contributor to nonlinear degradation in the radio equipment. The second most contributory circuit is the downconverter. Its nonlinearity is only of concern during normal or abnormally high signal level conditions and not during periods of fading.

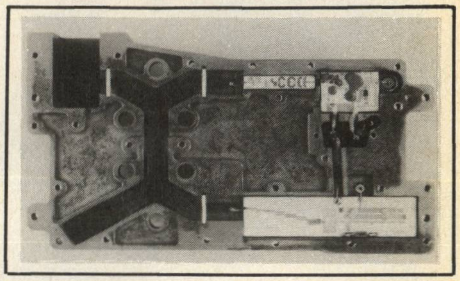

Fig. 5 6-GHz upconverter.

Radio Repeater Components

— Transmitter

Because a GaAs FET power amplifier is used at 6 GHz and a TWT is used at 11 GHz, the design considerations for the upconverters are somewhat different. For the solid-state amplifier at 6 GHz, gain is achieved by cascading discrete amplifier stages. Therefore, economy dictates that the upconverter be designed to produce as much RF power as is practical, and so the mixer uses a varactor diode. With a TWT amplifier at 11 GHz, 40 dB of gain is achieved directly, and thus the lower power upconverter uses a Schottky barrier diode. Figure 4 shows that both upconverters are single diode designs, wherein the signal and local oscillator are separated by a circulator. An isolator has been included to provide a good impedance match for the LO, and to terminate the unwanted sideband after its reflection from the sideband selection filter. Figure 5 is a photograph of the 6-GHz upconverter illustrating the variable gain IF amplifier, varactor mixer, circulator, isolator, and a step recovery diode frequency sextupler for the local oscillator. This circuit is representative of the microwave integrated circuit construction used throughout the repeater.

[Continued on page 76]

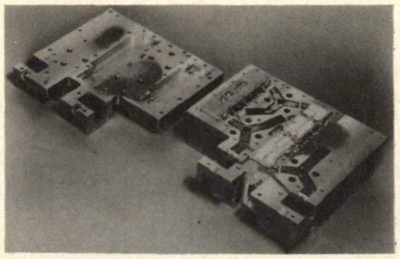

Fig. 6 6-GHz GaAsFET power amplifier.

The 6-GHz GaAs FET power amplifier shown in Figure 6 has four stages with a total gain of 30 ±3 dB and a saturated output power of about 4.5 watts (+36.5 dBm). This amplifier has well controlled gain and phase characteristics to within 1 dB of the saturation point. The amplifier can be operated at an average power of 30.0 dBm while producing intermodulation distortion at least 36 dB below the signal.[2,5] The 11 GHz TWT amplifier has a gain of 43 ±3 dB and a minimum saturated output power of 20 watts (±43 dBm). Unlike the GaAs FET amplifier, the TWT shows a significant gain and phase deviations at a power 10 dB below the saturation point. However, these nonlinearities are well described by a third power distortion model. Figure 7 shows a simple 70-MHz predistorter which allows the amplifier to be operated at +37 dBm and meet its distortion allocation. The predistorter circuit takes a sample of the 70-MHz signal, passes it through an expansive nonlinear amplifier (its gain increases with increasing input signal level), and adds the output to the main IF signal. The amplitude and phase of the distorted signal are adjusted to cancel the amplitude and phase deviations of the TWT.

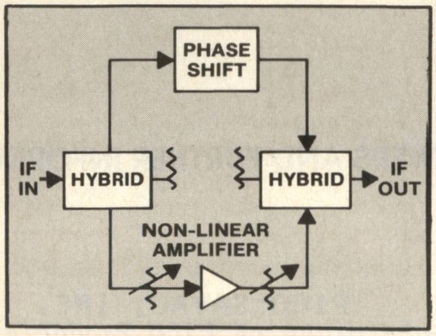

Fig. 7 Predistorter block diagram.

While the GaAs FET amplifier operates well at an average transmit power of +30.0 dBm, it degrades abruptly when the power is increased beyond this point. The amplifier gain is a function of temperature and, therefore, the transmitter has an automatic level control loop, which controls the gain of the IF driver in the upconverter, as indicated in Figure 2. With this arrangement, the output power is typically held constant to within ±0.1 dB over a temperature range of 0 to 50°C. In the 11-GHz transmitter, a similar leveling loop controls the output power to keep it constant with aging and temperature. This is necessary so that the TWT distortion products remain at a fixed level for cancellation by the predistorter ciruit.

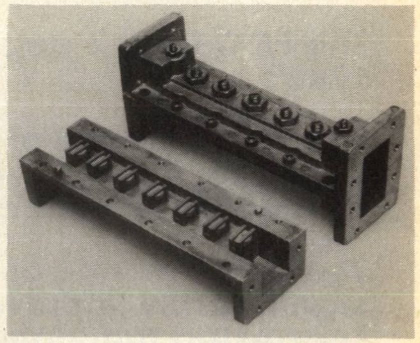

Fig 8 6-GHz barium titanate resonator filter.

— Microwave Networks

The channel combining and separating networks should contribute minimal amplitude or delay shape to the digital channel. Because of the high spectrum efficiency at 6 GHz (3 bits/Hz), the RF filter bandwidth is not large compared to the digital spectrum width. Therefore, these filters must be stable with temperature. This stability is achieved at 6 GHz by using barium titanate dielectric resonators mounted in cutoff waveguide (Figure 6).[6,7] The dielectric constant of this material is about 40 and the resonator Q is about 6000. A temperature stability comparable with that of an Invar waveguide filter is achieved, but the dielectric resonator filter is compact and inexpensive. The seven resonator filters are Butterworth designs with insertion losses of 1 dB and return losses in excess of 30 dB. These filters coupled with circulators form the 6-GHz channel combin-

[Continued on page 78]

[From page 76] **DIGITAL RADIO**

ing and separating networks. The five-resonator sideband selection filter between the upconverter and the power amplifier uses the same technology.

The channel separation is achieved at 11 GHz with waveguide directional filters.[8] Such filters contribute less loss than circulators to the "through" channels. A conventional waveguide filter is used for sideband selection.

— Receiver

Because DR-630 uses a low noise GaAs FET preamplifier in the 6-GHz common receiving waveguide run, it is convenient to define noise figure and system gain referenced to the input of this RF preamplifier. The 6-GHz 2 stage GaAs FET preamplifier (Figure 9) has a nominal gain of 15 dB and noise figure of 2.8 dB. An automatic bypass network limits the signal loss to 10 dB in case of device failure or power loss.[9] Locating this amplifier ahead of the channel separation filters has the advantage of masking the filter losses and blocking the image noise response. The use of a low noise preamplifier allows a broadband medium performance downconverter to be used. The mixing device is a Schottky barrier diode and the noise figure of the mixer plus IF preamplifier is about 10 dB. An overall receiver noise figure of 4 dB is achieved at 6 GHz.

At 11 GHz, the use of a high performance GaAs Schottky barrier diode with tuned image rejection results in a downconverter noise figure of 6.6 dB. The overall receiver noise figure including channel separation losses is 9 dB.

After conversion to the 70-MHz intermediate frequency, the signal is bandlimited and the envelope delay and amplitude imper-

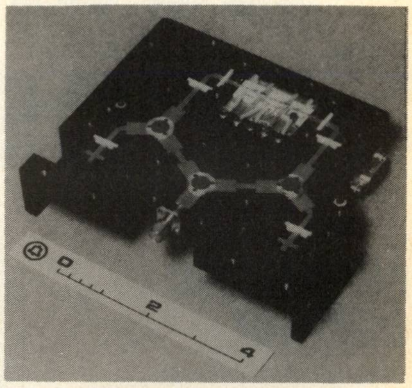

Fig. 9 Two stage 6-GHz RF preamplifier.

fections resulting from RF filtering are equalized.

The primary purpose of the IF main amplifier is to keep the receiver output power constant with varying propagation conditions. This amplifier, shown in Figure 10, has been realized as a thin film hybrid integrated circuit. It consists of four variable gain stages (each with 0 to 20 dB range) and an output driver stage. The use of high frequency transistors (f_T = 5 GHz) as feedback pair amplifiers results in a wideband device with excellent linearity. The gain control is obtained by using PIN diodes to vary the amount of negative feedback.

Odd-order amplitude shape associated with multipath propagation effects is the major contributor to outage of a digital radio systems.[10] A dynamic amplitude slope equalizer is used to reduce the first-order effect of amplitude slope

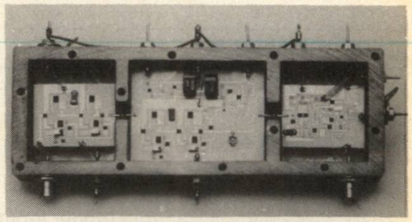

Fig. 10 70-MHz AGC amplifier.

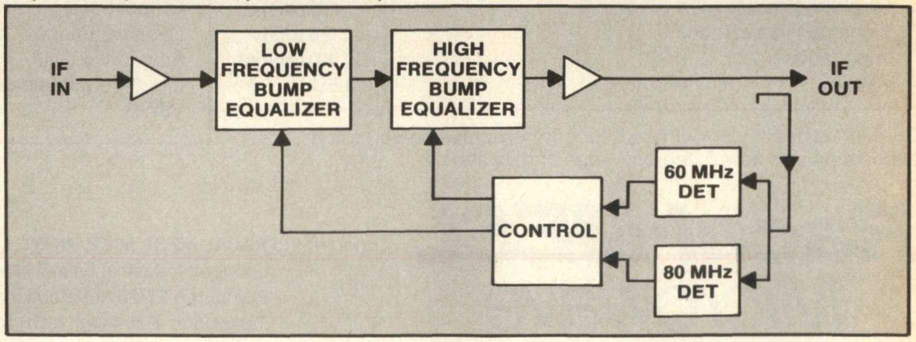

Fig. 11 Adaptive amplitude equalizer block diagram.

caused by selective fading. Figure 11 shows that the circuit depends on two frequency-separated samples of the received signal spectral density to control a pair of complementary bump equalizers. Amplitude slopes of ±10 dB over a 30-MHz band are reduced to ±1 dB by this circuit.

— Local Oscillators

Different design approaches were taken for the microwave local oscillators at 6 and 11 GHz. The same radio equipment used for DR 6-30 may also be used in a long haul-rated heterodyne frequency modulated system (FR 6-30). In such a system, carrier frequency errors accumulate and thus the individual oscillators must be very stable (approximately ±2 ppm). To obtain this accuracy, a 1-GHz transistor oscillator is phaselocked to a 4-MHz temperature compensated crystal oscillator, as shown in Figure 12. The 1-GHz region was chosen so that an available digital integrated circuit could be used to divide this frequency down to 4 MHz.

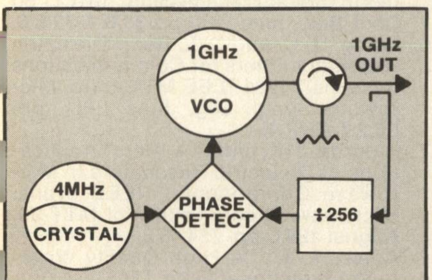

Fig. 12 1-GHz phase-locked oscillator block diagram.

The DR 11-40 radio has no companion heterodyne FM analog radio system. A regenerative digital system can tolerate larger frequency variations (about ±20 ppm), and so, the 11-GHz local oscillators are not crystal stabilized. Figure 13 shows a 3.7-GHz bipolar transistor oscillator stabilized by a temperature controlled barium titanate dielectric resonator.[7,11] The output of this oscillator is amplified to about +26 dBm by a single GaAs FET stage and multiplied to 11 GHz by a varactor tripler. Typically a frequency stability of ±2 ppm is achieved over a 0 to 50°C temperature range, leaving ample margin for aging effects.

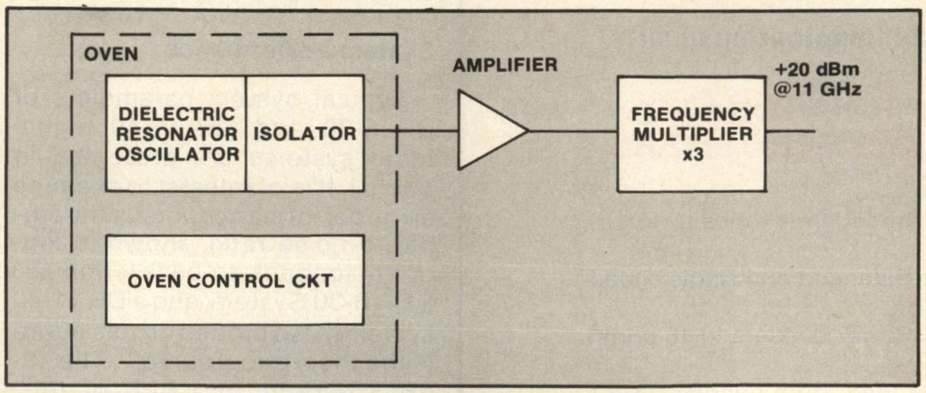

Fig. 13 11-GHz local oscillator block diagram.

TABLE I
IMPORTANT SYSTEM PARAMETERS

ITEM	DR 6-30	DR 11-40
Radio Frequency Band	5.925-6.425 GHz	10.7-11.7 GHz
Overall Bit Rate	90.524 Mb/s	90.524 Mb/s
Modulation Format	16-QAM	16-QAM
Transmitter Power (at the antenna port)	+29.0 dBm	+34.0 dBm
Noise Figure	4.0 dB (at RF Preamp input)	9.0 dB (at dropping filter input)
Receiver Threshold (typical at BER = 10^{-3})	-78 dBm	-73 dBm
System Gain (typical at BER = 10^{-3})	107 dB	107 dB

[Continued on page 80]

[From page 79]

Oscillators for digital radio service must not exhibit phase discontinuities. Such an event can cause loss of carrier recovery phaselock loop synchronization. To avoid these transient effects, each 1-GHz phaselocked oscillator is screened via temperature cycling, and each 11-GHz generator is aged and monitored for one week before system use.

System Performance

Typical systém parameters of DR 6-30 and DR 11-40 digital radio systems are presented in Table I. It is of interest to examine error performance versus the signal-to-noise ratio, shown in Figure 14 for back-to-back terminals, a DR 6-30 System, and a DR 11-40 system. Also plotted on this figure is the theoretical curve.[12] The 18-dB S/N ratio, at a BER of 10^{-3}, translates to a system gain of 107 dB, either with a 4-dB noise figure and +29 dBm transmitter power at 6 GHz or a 9-dB noise figure and +34 dBm at 11 GHz.

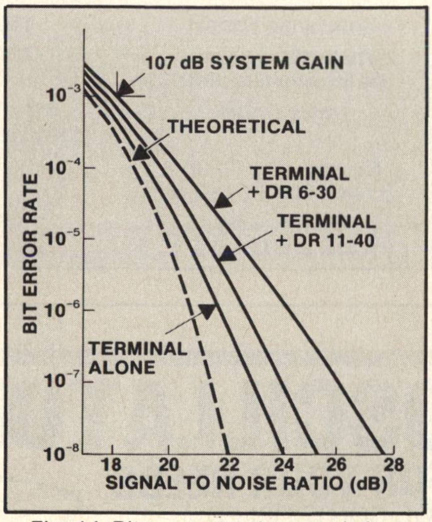

Fig. 14 Bit error rate characteristics.

The long term error rate performance (unstressed by thermal noise) of digital radio systems is important if data service is to be carried. This performance corresponds to the "tail" of the BER curve (BER $<10^{-9}$), corresponding to very large S/N ratios. Using a statistical model for system errors,[1] it is possible to show that the 21% eye opening to the 10^{-8} BER point of DR 6-30 predicts a long term system error rate of about 1×10^{-12}. Verification tests of the statistical error model on actual systems have shown this method to be a good predictor of the system long term error performance. Some additional degradation is expected from the amplitude and delay shape of the antenna system. However, experience has shown that a properly engineered antenna system will not degrade the long term error rate to less than 10^{-10}.

REFERENCES

1. Bates, C. P., A. C. Longton, K. L. Seastrand, and M. A. Skinner, "DR 6-30 System Design and Application," in ICC' 81 Conference Rec., June 1981, pp. 3.1.1-3.8.
2. Schwarz, W. J., R. P. Slade, and J. J. Kenny, "Radio Repeater Design for 16-QAM," in ICC' 81 Conference Rec., June 1981, pp. 13.5.1-13.5.7.
3. Kenny, J. J., "Impact of Inteference on 16-QAM System Requirements," in NTC' 80 Conf. Rec., December 1980, pp. 43.4.1-43.4.6.
4. Osborne, T. L., G. L. Frazer, G. L. Fenderson, and S. W. Hough, "In-Service Performance Monitoring for Digital Radio Systems," ICC' 81 Conf. Rec., June 1981, pp. 35.2.1.1-35.2.5.
5. Heiter, G. L., and R. R. Grady, "Measurement and Analysis of Nonlinearities in Digital Transmission," in ICC' 80 Conf. Rec., June 1980, pp. 33.6.1-33.6.6.
6. Wang, H. C. and C. L. Ren, "Dielectric Resonator Filters for Communications Systems," 1981 IEEE MTT-S Int. Microwave Symp. Dig, June 1981, pp. E6.2.1-E6.2.4.
7. Plourde, J. K, and C. L. Ren, "Applications of Dielectric Resonators in Microwave Components," IEEE Trans. Microwave Theory Tech., Vol. MTT-29, August 1981, pp. 754-770.
8. Abele, T. A., "A High Quality Waveguide Directional Filter," B.S.T.J., Vol. 46, No. 1, January 1967, pp. 81-104.
9. Knerr, R. H. and C. B. Swan, "A Low-Noise Gallium Arsenide Field Effect Transistor Amplifier for 4 GHz Radio," B.S.T.J., Vol. 57, No. 3, March 1978, pp. 479-490.
10. Giger, A. J. and W. T. Barnett, "Effects of Multipath Propagation on Digital Radio," 1980 International Zurich Seminar on Digital Communications, March 1980, pp. D2.1-D2.5.
11. Plourde, J. K., D. F. Linn, I. Tatsuguchi, and C. B. Swan, "A Dielectric Resonator Oscillator with 5 ppm Long Term Stability at 4 GHz," 1977 IEEE MTT-S Int. Microwave Symp. Dig., June 1977, pp. 273-276.
12. Prabhu, V. K., "The Detection Efficiency of 16-ary QAM," B.S.T.J., Vol. 59, No. 4, April 1980, pp. 639-656.

John J. Kenny, *received the BS degree in EE from the University of Rhode Island in 1963, and the MS and PhD degrees in EE from the California Institute of Technology in 1964 and 1968, respectively. Since joining Bell Telephone Laboratories in May 1968 as a Member of the Technical Staff, Mr. Kenny has been active in the study and design of analog and digital microwave radio systems.* ■

Microwave Analog Radio Design

M. P. Salas
Rockwell International
Collins Transmission Systems Division

Introduction

The MAR-6C is an all solid-state IF heterodyne microwave radio with a transmission capacity of up to 2400 message channels in the 5925 to 6425 MHz frequency band.[1] With a transmit power of +37 dBm and a receiver noise figure of 5 dB, the MAR-6C is able to meet the Bell long-haul noise requirements.[2] As shown in the simplified schematic of Figure 1, the basic MAR-6C radio consists of a transmit/receive subsystem configured as a through-repeater, i.e. the receiver output

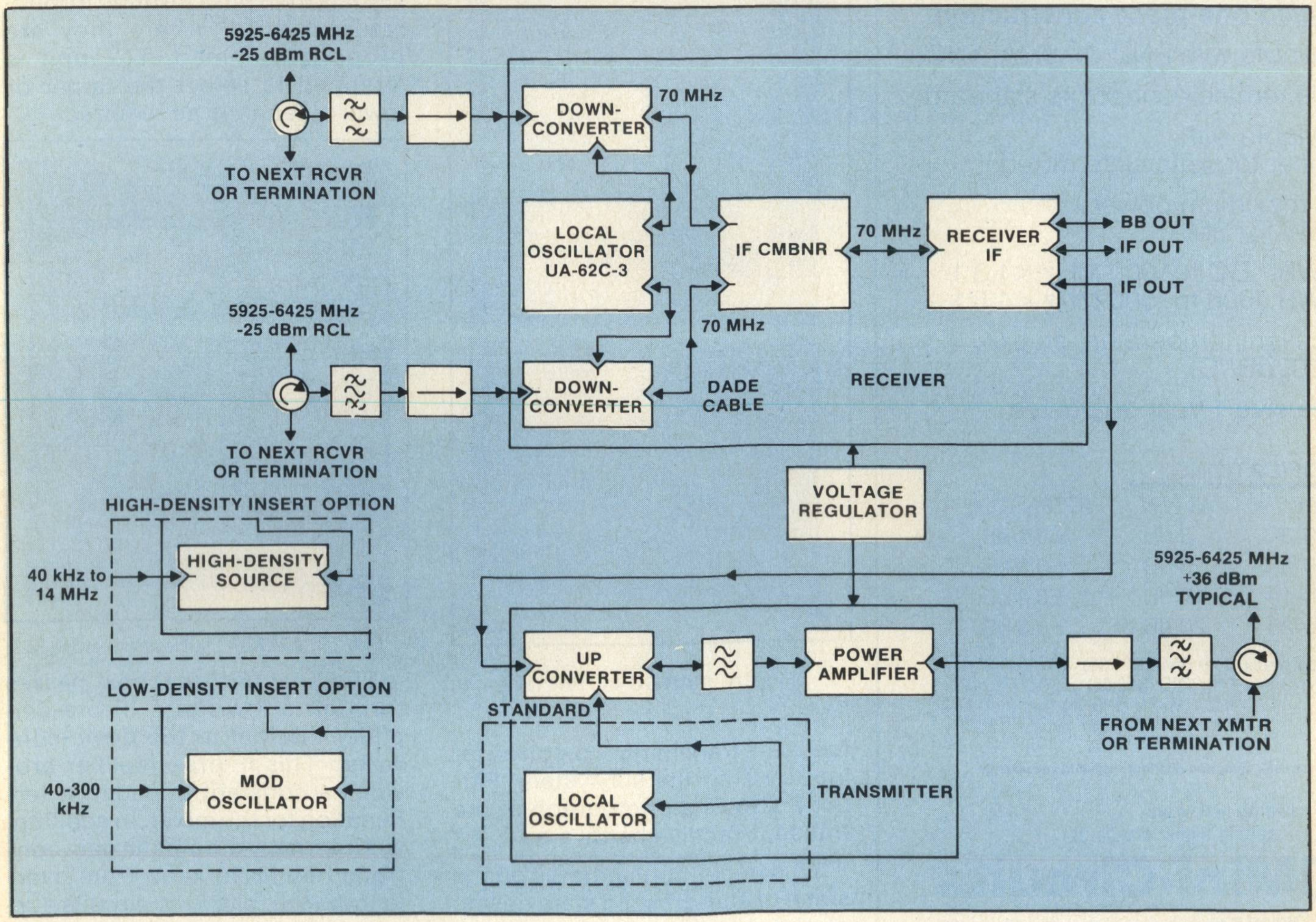

Fig. 1. MAR-6C simplified schematic.

[Continued on page 86]

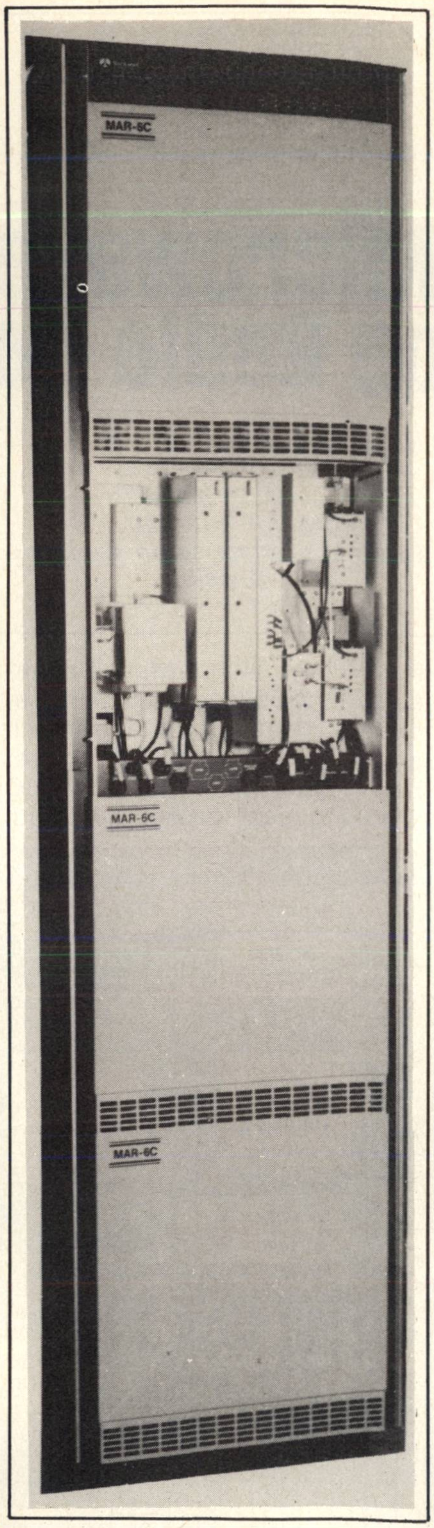

Fig. 2A. MAR-6C 4 T/R/R rack.

feeds the transmitter up-converter input within the subsystem. Figure 2 shows a photograph of the transmit/receive hardware.

This paper concentrates on the state-of-the-art solid state design of the microwave circuitry employed throughout the radio.

Microwave Module Descriptions

Down-Converter

The MAR-6C down-converter shown in Figure 3 provides a nominal 26 dB RF-to-IF gain and includes a GaAs FET low-noise amplifier (LNA) which sets the overall down-converter noise figure to 3.5 dB maximum. The LNA consists of a single stage with a nominal 10 dB gain and a 2 dB noise figure. A single adjustment optimizes the noise figure of the LNA in the center of the 5.9 to 6.4 GHz band, resulting in a unit that is broadbanded, i.e., no adjustments are necessary on any frequency used within this band.

The mixer itself is a single-sideband design.[3,4] This precludes the need for an image filter between the LNA and mixer, thus permitting the simple, compact broadband frequency design achieved. The mixer outputs two 70 MHz signals that are 90 degrees apart in phase. These two signals then pass through a quadrature hybrid, where they are properly summed. The unit is strapped to select the upper or lower sidebands as required.

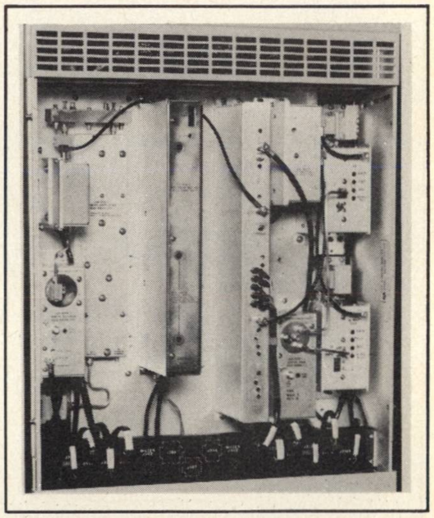

Fig. 2B. MAR-6C subsystem closeup.

The final IF signal next passes through a low-noise IF pre-amplifier internal to the down-converter. This IF pre-amplifier provides a constant impedance termination for the mixer. In addition, it is internally automatic gain controlled so as to keep from overloading the following circuits during up-fades or hot path conditions. By keeping the RF LNA

[Continued on page 88]

[From page 86]

gain at 10 dB, overloading of the input stage is virtually impossible.

Local Oscillator

The MAR-6C local oscillator (Figure 4) consists of a waveguide cavity containing a bipolar transistor used as the source of RF energy. The waveguide cavity is mechanically tunable over the full 5925-6425 MHz range. A sample of the RF output is coupled into the AFC circuitry, where it is mixed down to an intermediate frequency of approximately 25 MHz. This IF signal is then amplified and passed through a digital divider to a phase detector which generates an error voltage. This error voltage is filtered, amplified, and then applied to a varactor diode within the cavity so as to control the final cavity frequency.

The entire AFC, including the comb generator and microwave mixer, is contained on a G-10 printed circuit board. The 116 MHz crystal oscillator and doubler are contained on a single thick-film hybrid. The frequency of the L.O. is determined by the crystal frequency.

Up-Converter

The MAR-6C up-converter limits the incoming 70 MHz signal and then mixes it with the L.O. signal as shown in Figure 5. The 0 dBm, 70 MHz IF signal from the IF amplifier first passes through a buffer amplifier that has approximately 14 dB gain. The signal is then symmetrically limited, amplified to +14 dBm and applied to the mixer. Also included in the up-converter is a 70 MHz quieting oscillator. This is a simple crystal oscillator that is enabled by the receiver squelch alarm. When the receiver squelches, no 70 MHz signal is present. The quieting oscillator is enabled to keep the RF signal present. This is necessary since loss of the RF signal would cause receiver squelching in the next downstream receiver, i.e. RF continuity would be lost to the entire section.

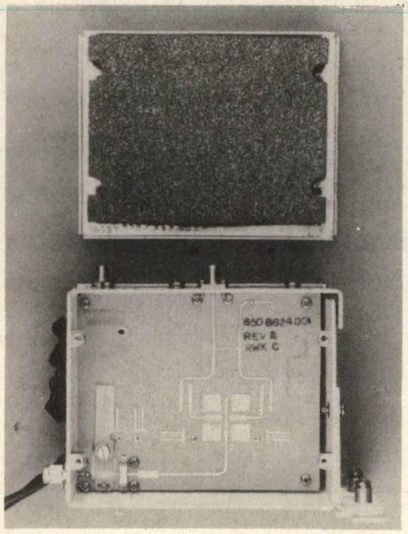

Fig. 3 MAR-6C LNA/SSB down converter.

The local oscillator signal for the up-converter reaches the mixer diodes by way of a balun (Figure 6).[4] Two of the diode terminals are connected to the two conductors making up the balanced line. The limited 70 MHz IF signal is fed to the diode center tap. The output dual balun then transforms the signal back to a single-ended configuration. This balun arrangement provides very good isolation properties. The pump signal is isolated from the mixer output, since the energy on the two conductors making up the balanced feed is 180 degrees out of phase, thereby cancelling at the diode center tap. In the other direction, the 70 MHz signal cannot propagate back through the balun since the balanced line is effectively at ground to the IF signal.

The RF isolation from the IF input is provided by an RF reject filter. This filter looks like an open circuit at RF, yet permits passage of the 70 MHz IF signal. The final RF output from the mixer contains both an upper and lower sideband. An external 4-pole coaxial filter is used to select the desired sideband. In addition, this filter also includes reject notches at plus and minus 70 MHz about the RF signal to eliminate the possibility of interfering tone in the next-to-adjacent downstream receiver.

A photograph of the up-converter is shown in Figure 7.

FET Power Amplifer

The MAR-6C FET power amplifier shown in Figure 8 provides a 37 dB power gain to the up-converted RF signal.

The 0 dBm frequency-modulated RF signal from the up-con-

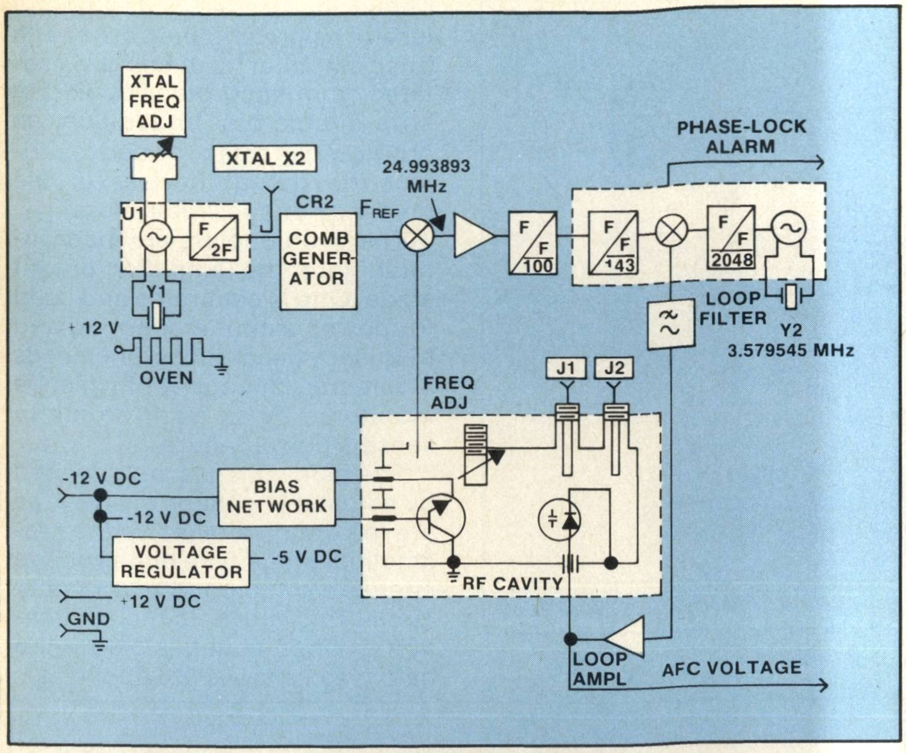

Fig. 4. MAR-6C local oscillator.

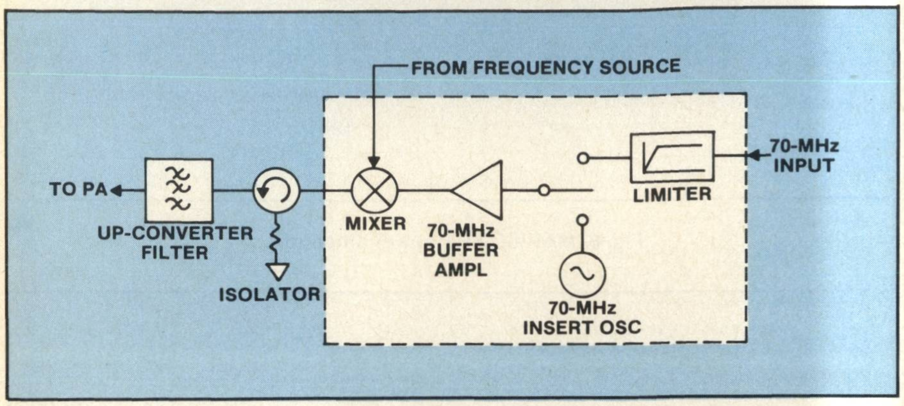

Fig. 5. MAR-6C up converter block diagram.

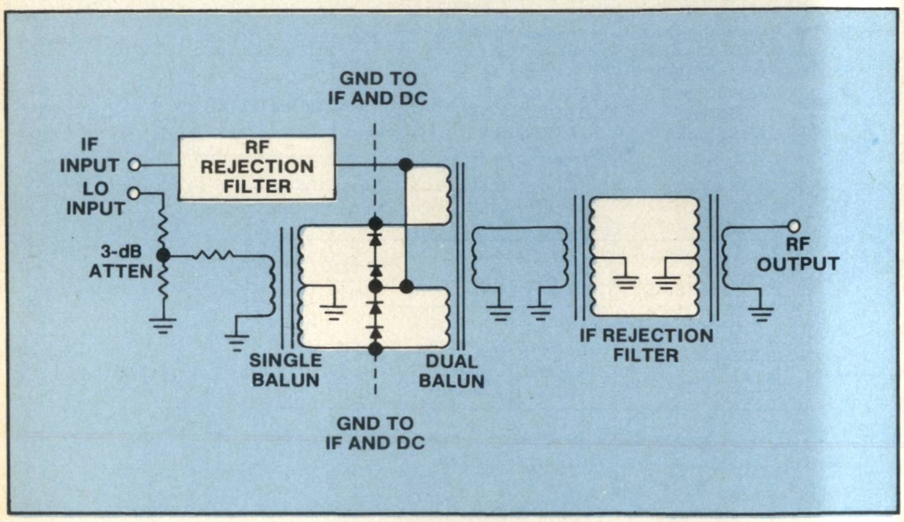

Fig. 6 Upconverter mixer balun.

[Continued on page 90]

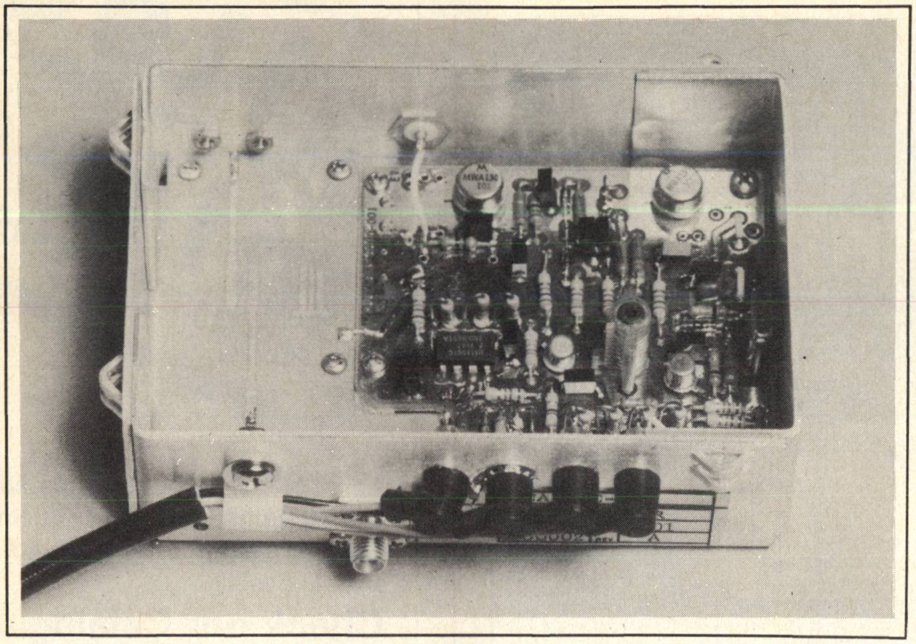

Fig. 7. MAR-6C upconverter.

verter enters the amplifier through the SMA input connector and is launched through a microstrip isolator to a 2-stage preamplifier. This preamplifier provides low-noise amplification with approximately 20 dB of gain. Another 14 dB of gain is provided by the following 2-stage driver amplifier. The driver ouput is fed to the final amplifier stage, where it is first split and then applied to the parallel 3 watt output FET's. The two outputs are combined in order to obtain the desired 5 watt output level. The preamplifier, driver and final amplifier sections are isolated from each other by microstrip circulators. In addition, an output isolator is provided to protect the output devices in the presence of poor return loss.

The two couplers are incorporated into the amplifier output stage. One is calibrated and used for power output monitoring and frequency checks. The other feeds a detector, the ouput of which is monitored by an alarm circuit to sense a power failure.

The gate voltages are provided by adjustable voltage dividers, as are the drain voltages on the preamplifier stage. The drain voltage circuits are equipped with a safety circuit that prevents the application of drain voltages before the gate bias voltages are applied.

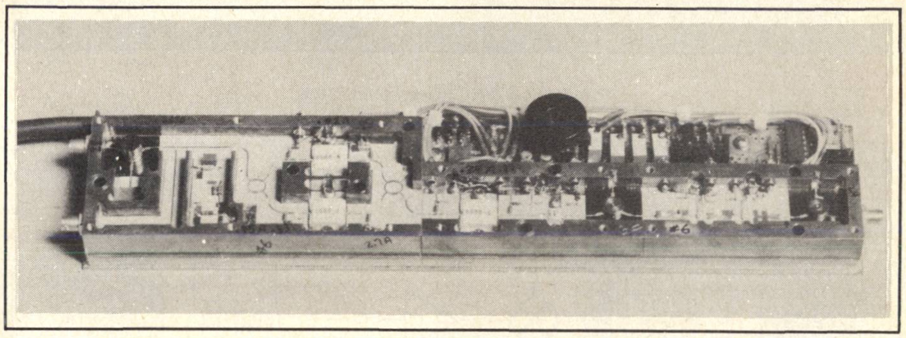

Fig. 8. MAR-6C FET power amplifier.

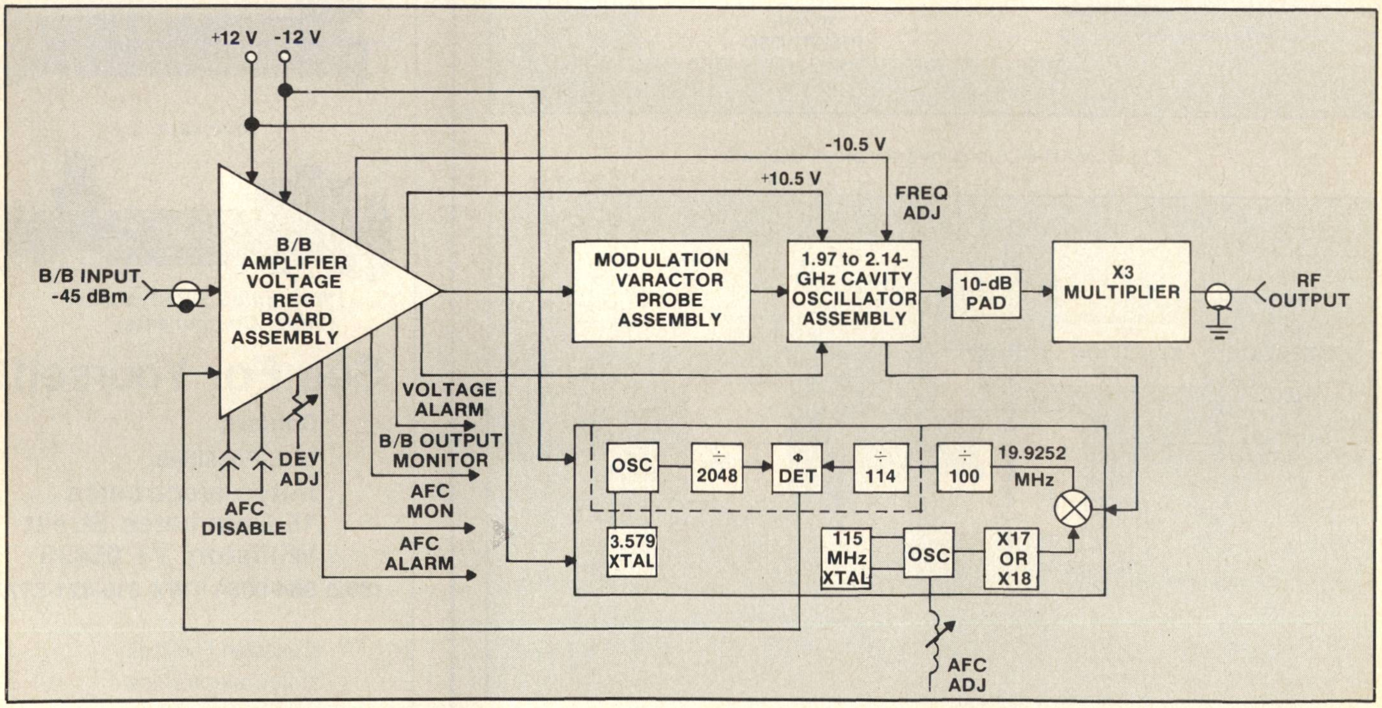

Fig. 9. MAR-6C high density source block diagram.

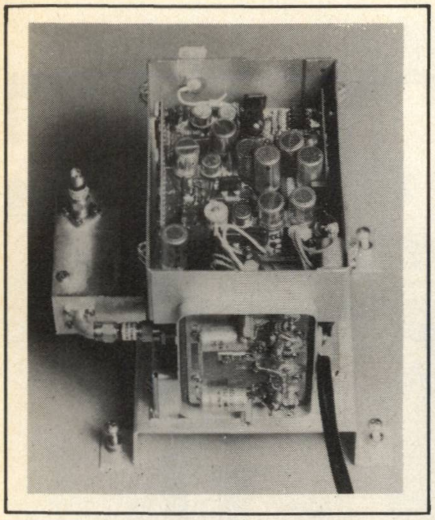

Fig. 10. MAR-6C high density source.

The FET power amplifier is a broadband unit. It covers the full 500 MHz band between 5925 and 6425 MHz.

Subbaseband Transmit Source

The MAR-6C subbaseband transmit source may be used in place of a local oscillator as a pump for the up-converter. It generates an RF signal and provides the means to modulate this RF signal with up to 60 channels in the 40 to 300 kHz range. This source incorporates the local oscillator as illustrated in Figure 3, with the addition of a modulating varactor in the oscillator cavity and an external subbaseband amplifier.

Subbaseband information in the 40 to 300 kHz range is applied to the unit at a nominal -45 dBm level through a 75 ohm connector. The signal is amplified, filtered, and finally applied to a modulation varactor in the RF cavity. Low noise amplification is required to keep the fixed noise of the source low. A 300 kHz active low-pass filter prevents harmonics of the subbaseband information from falling into the revenue carrying baseband of the radio. Also, the bias on this modulation varactor is adjusted to provide flat linearity, so the modulation varactor itself does not generate these unwanted harmonics.

High Density Transmit Source

The MAR-6C high density transmit source generates a signal in the 5925 to 6425 MHz band and provides the means to modulate this RF signal with a baseband signal comprised of up to 2400 channels. This source is typically used at terminals where it drives the power amplifier directly; and in an IF heterodyne transmitter at repeaters with high density drop and insert, where it drives the up-converter. Refer to Figures 9 and 10.

Baseband information in the 40 kHz to 14 MHz range is applied to the source at a -45 dBm nominal level. This information is first passed through a baseband amplifier, where it is amplified approximately 27 dB. The signal is then applied to the modulation varactor in the RF cavity. The baseband amplifier is dc-coupled. The dc bias voltages are monitored by a window detector, which generates an alarm should the bias point change.

The RF cavity itself operates between 1975 and 2142 MHz. A bipolar transistor is the source of RF energy. The source is run at an output level of approximately +27 dBm. This output level is padded down by 10 dB and then applied to a frequency tripler in order to achieve the final 6 GHz output frequency. The high level source, in conjunction with the pad, is necessary in order to provide isolation of the source from the tripler. Inadequate isolation causes source pulling, which degrades linearity and subsequently causes undesirable distortion.

Summary

The hardware aspects of the individual microwave modules comprising the Rockwell MAR-6C radio have been discussed. State-of-the-art designs were utilized in all cases resulting in units which combine high performance with low cost.

REFERENCES

1. Salas, M. P., "A new high capacity analog radio," National Telecommunications Conference, 1981, Session A5.3, November 29-December 3, 1981.
2. Salas, M. P., "High density FM systems," Rockwell International Transmission Engineering Symposium VI, March 29-April 1, 1982.
3. Hallford, B. R., "Single sideband mixers for communications systems," 1982 IEEE MTT-S International Microwave Symposium.
4. Hallford, B. R., "Simple balun-coupled mixers," 1981 IEEE MTT-S International Microwave Symposium. ■

Fiber Optics Marches into Microwave Systems

J. J. Pan
Harris Corporation
Melbourne, FL

Introduction

With the rapid growth of solid-state optoelectronics and optical fiber technologies, fiber-optic communications have progressed into gigabit (Gb/s) digital and microwave analog systems. Mutually advantageous enhancements in optical fiber and GaAs technologies make the evolution of microwave fiber-optic communications even more promising.

Despite the general trend toward digital transmission, there are attractive immediate potential applications for analog fiber-optic transmission due to its compatibiltiy with other existing analog transmission systems. The consideration to use analog transmission is further facilitated by such advantages as the narrower bandwidth required, the absence of complex timing and synchronization circuitry, and additional design and fabrication simplifications which could lower manufacturing cost and reduce system size and weight.

Microwave analog fiber optics have many applications, and as illustrated in Figure 1; most of these applications have been practically implemented. Commercially, multiplexed video signals and RF carrier transmission are well suited to satellite communications terminals[1] and microwave radios while fiber-optic sensors provide several unique advantages. For example, using a laser diode (LD) transmitter and an avalanche photodetector (APD) or metal semiconductor field-effect transistor (MESFET) receiver, the wideband fiber-optic link is capable of transmitting more than 20 channels of high-quality video signals. Both CATV[2] and C-band TVRO have been demonstrated using fiber cable. Conceivably, the analog fiber-optic link could also become attractive in conjunction with K-band (12 GHz) TVRO and high-definition TV channels, as well as with the Satellite Business Systems (SBS).

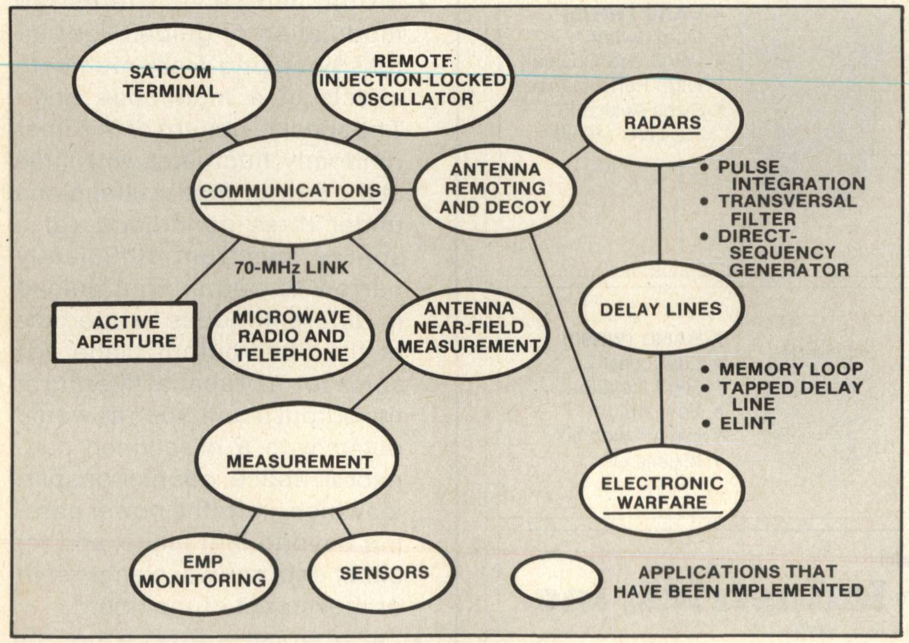

Fig. 1. Major microwave fiber-optic applications.

In military applications, jamming-resistant, spread-spectrum microwave and millimeter-wave communications and target acquisition systems, for example, can directly transmit information at RF carrier frequency through fiber cable with favorable signal-to-noise ratio (S/N) and dynamic range while minimizing transmission losses. The microwave fiber-optic link is also practical for electronic countermeasures (ECM) and radar signal processing.[4] One application of the microwave fiber-optic Electronic Intelligence (ELINT) is to link the antenna/low-noise front end and the channelized receiver, using the fiber-optic cable's large bandwidth to preserve the information fidelity of incoming signals and prevent undesirable EMI and common grounding problems.

System Design Criteria

For the same transmission quality the analog system requires a larger S/N than it digital counterpart. Therefore, S/N optimization over the operational bandwidth deserves special attention in analog system design. There are four basic noise sources associated with the fiber-optic microwave transmission channel,[5] which are:

- Laser Noise — Total LD intensity fluctuations caused by optical reflections from laser/fiber and fiber/fiber interfaces

TABLE 1. DESIGN CONSIDERATIONS FOR REDUCING LD NOISE

NOISE TYPE	NOISE REDUCTION APPROACHES
Laser Noise	Use of an optical isolator
	Reduction of the coupling efficiency between the LD and the optical fiber
Partition Noise	Use of a single-mode LD
Modal Noise	Use of a single-mode fiber (preferable)
	Use of a multimode fiber with large number of modes (next best alternative) and of an LD with broad spectrum width (multimode)
	Optimization of coupling between fiber and photodetector
	Improvement of connector and splice alignments
	Reduction of the total number of connectors, splices, couplers and splitters
Delay Noise	Thermal stabilization of LD
	Use of a broadband optical fiber

back into the laser resonator. This noise is phase, amplitude and frequency dependent.

- Partition Noise — Individual wavelength intensity fluctuations with constant total spectral intensity. As a multimode laser is modulated, the intensity of each wavelength can fluctuate, redistributing its energy to other modes. Contributing factors are (a) multimode (longitudinal) emissions from the laser, (b) individual mode amplification fluctuations, and (3) wavelength dependent losses within the transmission channel. Modal intensity perturbations are influenced by laser thermal conditions, signal reflections into the LD resonator, aging, operating point, and other LD-related conditions.
- Modal Noise — Undesired modulation of guided light intensity arising from multipath effects in a multimode fiber. The speckle pattern of this fiber randomly fluctuates with time at the output spatial filter plane under three conditions: (a) a source spectrum sufficiently narrow to permit light guided in different modes to interface at the fiber output plane, (b) some form of spatial filtering at the output plane, such as would occur with a misaligned connector, splice, coupler or splitter which limits the power passing beyond that plane, and (c) either a source wavelength shift or movement of the fiber.
- Delay Noise — Jitter in the time of arrival of optical pulses

transmitted through long optical fibers. This delay noise may significantly deteriorate the bit error rate of high-data rate systems.

Both electronic compensation and optical feedback methods have been applied to minimize LD noise sources. However, neither of these is practical for high-frequency, long distance operation. Some system design considerations for efficiently reducing LD noise are given in Table 1. The best approach in microwave fiber-optic design is to use the combination of a temperature stabilized single-mode LD, a single-mode fiber cable, and an optical isolator.

Performance of wideband analog fiber-optic systems is also sensitive to nonlinear distortion, delay distortion, system frequency response flatness, and impedance matching. Component nonlinearities cause harmonic and intermodulation product (IMP) distortions, and inadequate delay and gain flatness cause AM-to-PM conversion. The impedance matching of the fiber-optic transmitter/receiver circuit design determines system input/output VSWR's, noise and their modulation and detection efficiencies.

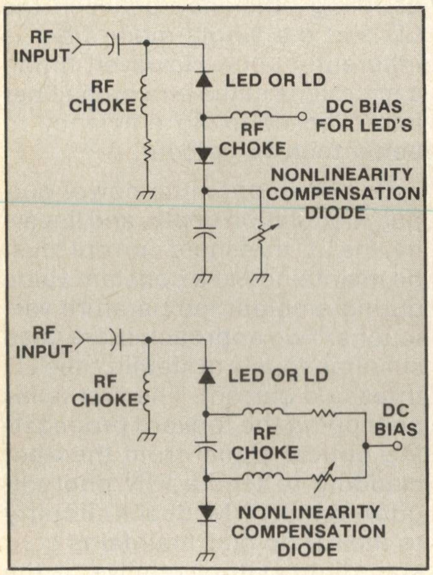

Fig. 2. Diagram of "Antiseries" compensation to reduce LD and LED nonlinearity.

Nonlinearity of fiber-optic systems arises from the LD, the LD driver, and the postdetector amplifier. Proper transistor selection and circuit design can significantly improve the linearity of an LD driver and postdetector amplifier. Inherent nonlinear junction capacitance, power versus current relationship, and thermal gradient of the LD, all create undesired harmonics and IMP's. All linearization approaches such as feedback, feedforward,[6] quasi-feedforward,[7] balanced compensation,[8] and circuit predistortion[9] require precision fabrication processes or expensive device characterization. An inexpensive "antiseries" push-pull technique[10] has been used to reduce LD nonlinearity. As depicted in Figure 2, a compensation diode of opposite polarity is inserted in RF series with the LD. The direct currents through the diodes are in parallel and are independently adjustable. Without linear compensation, the second and third-order IMP's of a two-tone test were 24 dB below the carrier, while with the compensation network, IMP's better than 60 dB below the carriers were obtained. [Continued on page 96]

Either a high-speed APD or a MESFET is suitable as the microwave photo-detector. The MESFET offers the advantages of low noise, low bias voltage, wide operational bandwidth, moderate amplification gain of approximately 10 dB, and high dynamic range,[11] while the APD has a relatively high gain of approximately 20 dB. Since the multiplication gain of APD varies with ambient temperature and bias voltage, a temperature/voltage stabilization circuit should be included in the wideband fiber-optic receiver design. The optimization of the receiver noise performance, gain flatness, output VSWR, and phase linearity can be accomplished using CAD techniques.

Microwave Fiber-Optic Systems

By applying the previously described principles of noise reduction and nonlinearity minimization, in conjunction with the practical technologies of source-fiber coupling efficiency improvement and temperature compensation, several microwave fiber-optic systems have been fabricated at the Harris Corporation.

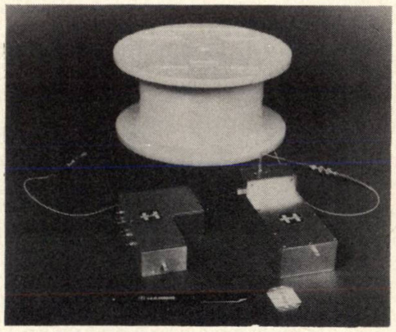

Fig. 3. 5-GHz transmitter and receiver linked by optical fiber cable with single amplifier stage shown in foreground.

5 GHz Fiber-Optic Link

At the leading edge of microwave fiber-optic technology, an unprecedented 5.0 GHz fiber-optic system which uses a 1 km single-mode fiber for antenna remoting and decoy applications has been demonstrated and is shown in Figre 3. A fast-response, single-mode LD is the optical source, while a silicon APD, mounted in a microwave package, having a response time of less than 100 picoseconds (ps) serves as the photodetector.

The 5 GHz wideband LD transmitter and APD receiver circuits are designed and optimized using measured device data. A computer-controlled network analyzer measures the impedance of the LD, APD, and MESFET over the 4.0 to 5.0 GHz frequency range at various bias conditions. However, great care must be exercised to eliminate or account for other factors which can cause measurement error, such as variations of LD threshold current and APD multiplication gain as a function of temperature.

The GaAs MESFET is ideally suited for use as a current driver for the microwave LD transmitter. The first-stage, low-noise MESFET driver amplifies the incoming RF signal to obtain the required modulation index, while the second-stage driver provides current amplification and LD impedance matching from 50 Ohms to 4 Ohms. These driver stages are fabricated in a microstrip configuration on alumina substrates. To reduce nonlinearity, an antiseries push-pull circuit, described previously, is incorporated in transmitter design.

Due to a number of factors, coupling efficiency between the LD and the single-mode fiber is inherently poor. However, fitting a microlens at the end of the fiber improved coupling efficiency to better than 15 percent.

To obtain optimum power output, modulation depth, and linearity, the LD threshold current must be maintained at a constant value during ambient temperature variations. Two approaches are used simultaneously to stabilize the LD threshold current. The first relies on tapping the forward propagating optical signal from the fiber cladding to feed a PIN photodiode monitor. A feedback circuitry to the LD dc bias maintains constant light output relative to the reference channel. The second approach uses a thermistor directly under the LD to sense temperature changes. Its output is routed through appropriate control circuitry and back to control the thermal electric cooler, and thus the LD bias current.

A microwave packaged APD with extremely fast response time serves as the detector in the receiver. The APD requires thermal compensation because its multiplication gain is also a function of temperature.[6] The APD is impedance matched to the low-noise MESFET post-detection amplifier stages to ensure low noise, low mismatch loss, low distortion, and wideband operation.[11]

A 1 km, single-mode optical fiber cable with 2.1 dB loss at 840 nm has been used for 5 GHz transmission with a 600 MHz bandwidth. The initially obtained 50 dB S/N in a 100 kHz window was instrumentation limited, and therefore the obtainable performance is expected to be substantially better.

700 MHz Fiber-Optic Link

A 700 MHz fiber-optic link with a 500 MHz bandwidth has been fabricated for spread-spectrum military SATCOM integrated terminal applications.[12] Basic components of the link are the LD transmitter, APD receiver, and 1 km of graded index fiber with a 3 dB bandwidth of 1825 MHz and a loss of less than 3 dB at 860 nm.

One critical basis for LD selection is that its output be free from kinks. Kinks are nonlinearities in LD output power versus current characteristics, and are caused by interactions between the laser modes. To prevent these nonlinearities and improve reliability, the LD must have a narrow stripe width of 5 μm or less.[13,14] Additional considerations were:

- Low threshold current
- Temperature effects
- Output power
- Frequency response

The selected device had no perceivable kinks, a threshold current of 30 mA, a modulation depth of approximately 70 percent, and a coupling efficiency of 20 percent based on a facet power of 2 mW. The transmission bandwidth extended from 450 to 1000 MHz and was limited at these points by the LD driver amplifiers. Thin-film amplifiers were chosen for their low noise and high intercept point. To minimize mismatch losses, the LD was impedance matched to the 50 Ohm driver amplifier.

The LD transmitter features a precision 3-axis adjustment scheme for optimizing LD/fiber alignment. The same cladding mode tap approach used in the 5 GHz system was applied to compensate LD output power as well as threshold current over temperature.

The fiber-optic receiver parameters are selected for the desired system performance characteristics: noise level, link sensitivity, bandwidth, and dynamic range. An APD for this application must have a low noise equivalent power (NEP), large active area, fast response time, and relatively low bias voltage.[15] The one chosen for the 700 MHz link has an NEP of 1×10^{-14} Watt/$\sqrt{\text{Hz}}$, an active area of 3×10^{-2} square millimeters, a rise time of less than 500 ps, a breakdown voltage of approximately 150 Volts, a gain-bandwidth product of about 800 GHz, and a quantum efficiency of approximately 77 percent. An impedance matching network interfaces the APD to four thin-film output amplifier modules which are chosen so that the first stage has a low noise figure and the last stage has a high intercept point to minimize IMP.

The complete link performed as follows:

- ±1.1 dB frequency response flatness across the 450 to 1000 MHz band
- 53 to 58 dB S/N in a 300 kHz bandwidth
- No measurable IMP at a -40 dBm input level

70 MHz Fiber-Optic Link

High-performance 70 MHz fiber-optic links have been used in conjunction with military and commercial microwave radios, radars, and satellite terminals. These 70 MHz links with a bandwidth of up to 40 MHz offer the well known advantages of fiber-optic transmission, particularly immunity to interference, low delay distortions, ease of installation, increased communication security, cost effectiveness, and high reliability. The fiber-optic system used with the Geostation-

[Continued on page 98]

ary Operation Environmental Satellite (GOES) earth station,[16] for example, was installed in 1976 and has proven to be extremely reliable.

The GOES fiber-optic link interconnects the downconverter and PSK receiver of 67.1 MHz with 8 MHz bandwidth over 3,000 feet of low-loss, graded index single fiber cable. The link uses a LED transmitter and an APD receiver.

The transmitter incorporates commercially available 50 Ohm driver amplifiers ahead of the LED. To obtain optimum modulation depth, an impedance transformer connects the final 50 Ohm driver to the low-impedance LED. In addition to a gain equalization circuit, the transmitter also uses the same type of nonlinear compensation circuitry mentioned earlier and a hyperbolic microlens at the fiber end to improve the coupling efficiency.

In the receiver, low noise and flat frequency response are of prime importance. The overall noise figure of the receiver is determined by the quantum noise generated by the APD and the noise figure of the post-detection amplifier. By compensating for APD admittance and matching it to the 50 Ohm output amplifier modules, flat frequency response and optimum noise figure are achieved.

Using a gain equalization circuit in the LED transmitter, the GOES link achieves a $S/N \geqq 42$ dB measured in a 100 kHz bandwidth. The nonlinearity compensation network secures a two-tone IMP of 60 dB below the carrier. The substantial progress made since 1976 in optical source power and fiber attenuation would currently make it possible to operate the GOES link over a distance of 2 km with a S/N in the 65 to 70 dB range.

Conclusion

The remarkable progress of wideband optical fiber offers very attractive opportunities for high-quality microwave signal transmission. Reducing the LD nonlinearity and noise has been instrumental in obtaining the required performance characteristics for analog fiber-optic links. Applications include multi-channel CATV, TVRO, secure microwave RF carrier transmissions, ECM, radar signal processing and sensor arrays.

Acknowledgments

The author would like to express his gratitude to M.J. Russell and M.G. Kunz for their assistance in preparation of this article.

REFERENCES

1. Pan, J.J., 1 GHz, "1 km fiber-optic line for satellite communication integration terminals," 1981 International Communications Conference, June 1981, Denver, Colorado.
2. Baack, C. et al, "Analogue optical transmission of 26 TV channels," *IEE Elect. Lett.*, 10 May 1979, pp. 300-301.
3. News, "TVRO receiver system uses two fibers," *Microwaves*, July 1981, p. 26.
4. Pan, J.J., "Fiber optics for microwave signal processing," SPIE Symposium on Effective Utilization of Optics in Radar Systems, September 1977, Huntsville, Alabama.
5. Miskovic, E.J., "Optical transmission channel noise phenomena for high bit fiber-optic systems," Electro-Optics laser '79 Conference, Anaheim, California.
6. Pan, J.J., "Temperature effects on military fiber-optics systems," Military Electronics Expo '78, Anaheim, California, 14-16 November 1978.
7. Straus, J., et al, "Phase-shift modulation of optical transmitters by a quasi feed forward compensation technique," *Elect. Lett.*, 17 March 1977, pp. 158-159.
8. Straus, J. and O.I. Szentiesi, "Linearization technique for linearization of analog optical transmitters," *Elect. Lett.*, 3 March 1977, pp. 149-150.
9. Asatani, K. and T. Kimura, "Linearization of LED nonlinearity by predistortions," *IEEE Trans. on Elect. Devices*, February 1978, pp. 207-212.
10. U.S. Patent 4,032,802
11. Pan, J.J., "Microwave fiber-optic communications systems," 1981 National Telecommunications Conference, 29 November 1981, New Orleans, Louisiana.
12. Pan, J.J., and M.G. Kuna, "1 GHz, 1 km fiber-optic link for satellite communication integrated terminals," FOC '81 East, 24-26 March 1981, Boston, Massachusetts.
13. Lang, R., "Literal transverse mode instability and its stabilization in strip geometry injection lasers," *IEEE Journal*, Quantum Electronics, August 1978, pp. 718-726.
14. Asbeck, P.M., et al, "Literal mode behavior in narrow stripe lasers," ibid, p. 727.
15. Pan, J.J., "Advanced photodetectors for fiber-optic communications systems," NEPCON '79, Anaheim, California, February 1979.

Pan, J.J., and D.E. Hailey, "Fiber-optic links for microwave and satellite communication terminals," National Telecommunication Conference, November 1976, Dallas, Texas. ■

Calculator Program for Impedance Matching

Wilfred J. Remillard
Dept. EE Northeastern University
Boston, MA

Introduction

When one first encounters the concept of impedance matching by means of adding a series section to a transmission line, he usually employs the quarter-wavelength technique. If the characteristic impedance of the line is Z_0 and the impedance to be matched is $Z_R = R_R + jX_R$, then the characteristic impedance of the matching section Z_1 will be the geometric mean of Z_0 and Z_R,

$$Z_1 = \sqrt{Z_0 Z_R} \quad (1)$$

and the length of the section will be a quarter of a wavelength. This technique is described in most texts on transmission lines[1,2], and in many texts on acoustics[3,4]. One finds, however, that Z_R is usually complex (i.e., it has both resistive and reactive parts). Thus, Z_1 will also be complex. Since most transmission lines and acoustic material have *real* characteristic impedances, this technique is not practical.

To produce a real value for Z_1 another method is often used. The added quarter-wavelength section is not connected directly to Z_R but is inserted in the line a distance from Z_R such that the impedance looking in toward the load at this point is real, say R. Then

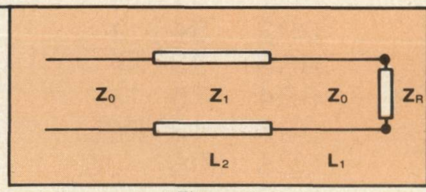

Figure 1
Series matching section Z_1 in line Z_0.

$$Z_1 = \sqrt{Z_0 R} \quad (2)$$

which gives a real value for Z_1 if Z_0 is real. . . as it usually is. The trouble with this method is that we cannot always find a line or acoustic material with characteristic impedance equal to Z_1.

Regier[5,6] takes a third approach, the one we will describe in this paper. In this method one has Z_0, Z_R, and Z_1 and attempts to determine the length of the section L_2 (in wavelengths) and the distance L_1 (in wavelengths) from Z_R. It should be noted that not all combinations of Z_0, Z_R, and Z_1 will lead to a feasible solution. The TI-59 calculator program presented in this article determines L_1 and L_2 (Figure 1), and it also indicates if the input data will lead to a feasible solution.

Design Equations[6]

We first normalize the real and imaginary parts of the load impedance, and the characteristic impedance of the line.
Thus,

$$r = R_R/Z_0 \quad (3)$$
$$x = X_R/Z_0 \quad (4)$$
$$z_1 = Z_1/Z_0 \quad (5)$$

We then determine the intermediate quantities

$$B = \{[[r-1)^2+x^2]/[r(z_1-1/z_1)^2 -(r-1)^2-x^2]\}^{1/2} \quad (6)$$

and

$$A = [(z_1-r/z_1)B+x]/[r+z_1B-1 \quad (7)$$

Finally, the required lengths, L_2 and L_1 are obtained from

$$L_2 = (\tan^{-1} B)/2 \quad (8)$$
$$L_1 = (\tan^{-1} A)/2 \quad (9)$$

Equations (3) through (9) can now be used to write a computer or a calculator program to determine L_2 and L_1 given R_R, X_R, Z_1, and Z_0. In the next section we will

```
000  76 LBL
001  11  A          058  54  )          115  76 LBL
002  42 STO         059  42 STO         116  16 A'
003  01  01         060  08  08         117  53  (
004  91 R/S         061  53  (          118  53  (
```

005	76	LBL	062	53	(	119	53	(
006	12	B	063	43	RCL	120	43	RCL
007	42	STO	064	05	05	121	07	07
008	02	02	065	65	×	122	75	-
009	91	R/S	066	53	(	123	43	RCL
010	76	LBL	067	43	RCL	124	05	05
011	13	C	068	07	07	125	55	÷
012	42	STO	069	75	-	126	43	RCL
013	03	03	070	01	1	127	07	07
014	91	R/S	071	55	÷	128	54	)
015	76	LBL	072	43	RCL	129	65	×
016	14	D	073	07	07	130	43	RCL
017	42	STO	074	54	)	131	11	11
018	04	04	075	33	X²	132	85	+
019	91	R/S	076	75	-	133	43	RCL
020	76	LBL	077	53	(	134	06	06
021	15	E	078	43	RCL	135	54	)
022	43	RCL	079	05	05	136	55	÷
023	02	02	080	75	-	137	53	(
024	55	÷	081	01	1	138	43	RCL
025	43	RCL	082	54	)	139	05	05
026	01	01	083	33	X²	140	85	+
027	95	=	084	75	-	141	43	RCL
028	42	STO	085	43	RCL	142	06	06
029	05	05	086	06	06	143	65	×
030	43	RCL	087	33	X²	144	43	RCL
031	03	03	088	54	)	145	07	07
032	55	÷	089	55	÷	146	65	×
033	43	RCL	090	43	RCL	147	43	RCL
034	01	01	091	08	08	148	11	11
035	95	=	092	95	=	149	75	-
036	42	STO	093	35	1/X	150	01	1
037	06	06	094	70	RAD	151	54	)
038	43	RCL	095	77	GE	152	54	)
039	04	04	096	17	B'	153	22	INV
040	55	÷	097	91	R/S	154	30	TAN
041	43	RCL	098	76	LBL	155	77	GE
042	01	01	099	17	B'	156	18	C'
043	95	=	100	34	√X	157	85	+
044	42	STO	101	42	STO	158	89	π
045	07	07	102	11	11	159	95	=
046	53	(	103	22	INV	160	76	LBL
047	53	(	104	30	TAN	161	18	C'
048	43	RCL	105	55	÷	162	55	÷
049	05	05	106	53	(	163	53	(
050	75	-	107	02	2	164	02	2
051	01	1	108	65	×	165	65	×
052	54	)	109	89	π	166	89	π
053	33	X²	110	54	)	167	54	)
054	85	+	111	95	=	168	95	=
055	43	RCL	112	42	STO	169	42	STO
056	06	06	113	12	12	170	13	13
057	33	X²	114	91	R/S	171	91	R/S

Figure 2 TI-59 calculator program for impedance matching.

present a program for performing this task on a TI-59 calculator.

Calculator Program

The program listing is given in Fig. 2. To run this program enter the value Z_0 for the characteristic impedance of your line, then press A. Next enter the real part of Z_R and press B. Follow this by entering the imaginary part of Z_R and press C. Next enter Z_1 and press D. Finally, when you press E, L_2 will be displayed, and when you press A′, L_1 will be displayed. If a set of values for Z_0, R_R, X_R, and Z_1 is chosen which does not allow a feasible solution, then L_2 will be displayed as a negative number.

Example

In this example, $Z_0 = 100$, $Z_R = 80 + j20$, and $Z_1 = 70$. Enter 100 and press A; enter 80 and press B; enter 20 and press C; enter 70 and press D. Finally, when you press E, L_2 will be displayed as .0714558420, and when you press A′, L_1 will be displayed as .0159902472.

If in the above example we had used Z = 90 instead of 70, the value for L_2 would be displayed as a negative number, indicating that you cannot use a 90-ohm section of line to match the given load to the 100-0hm line.

Conclusions

Regier's method is difficult to implement with Smith charts as it requires the use of the chart in its unfamiliar off-center mode[5]. Because the program presented is easy to use, and the results are very accurate, it should be useful to microwave engineers and acousticians. The program has been thoroughly checked for correct and accurate results.

REFERENCES

1. Johnson W., "Transmission Lines and Networks", McGraw-Hill (1950).
2. Seshadri S., "Fundamentals of Transmission Lines and Electromagnetic Fields", Addison-Wesley (1971).
3. Kinsler L. and A. Frey, "Fundamentals of Acoustics", (second edition), John Wiley and Sons (1962).
4. Temkin S., "Elements of Acoustics", John Wiley and Sons (1981).
5. Regier F.A., "Series-Section Transmission-Line Impedance Matching", QST, pp. 14-16 (July 1978).
6. Regier R.A., "Impedance Matching with a Series Transmission Line Section", Proceedings of the IEEE, pp. 1133-1134 (July 1971). ■

217 GHz Phase-Locked Impatt Oscillator

J. M. Cadwallader, M. M. Morishita and H. C. Bell
Hughes Aircraft Company
Electron Dynamics Division
Torrance, CA

A stable, low-noise phase-locked millimeter-wave IMPATT oscillator operating at 217 GHz was developed. The system utilizes a state-of-the art CW IMPATT millimeter-wave source to generate the required output power and frequency, and a low frequency stable crystal controlled reference oscillator and associated electronics to precisely phase lock the millimeter-wave source.

Introduction

Millimeter-wave systems development has become increasingly important and active in recent years. The key elements required for systems are millimeter-wave sources. IMPATT oscillators have already been developed and operated at frequencies beyond 200 GHz.[1] Many systems require stable, low-noise sources.[2] To meet the requirement, we have recently developed a phase-locked IMPATT oscillator operating at 217 GHz.

A simplified block diagram of the phase-locked system is shown in Figure 1. A bias-tuned CW IMPATT VCO provides the system's output signal F_{RF} at a nominal 217 GHz which is sampled at the crossguide coupler and fed to the RF port of the harmonic mixer. At the harmonic mixer this signal is mixed with the twelfth harmonic of a local oscillator signal F_{LO} at about 18 GHz and heterodyned down to a VHF intermediate frequency F_{IF} of about 100 MHz. The 18-GHz local oscillator signal F_{LO} is derived from a high-stability VHF reference crystal oscillator F_R, and a phase-locked microwave

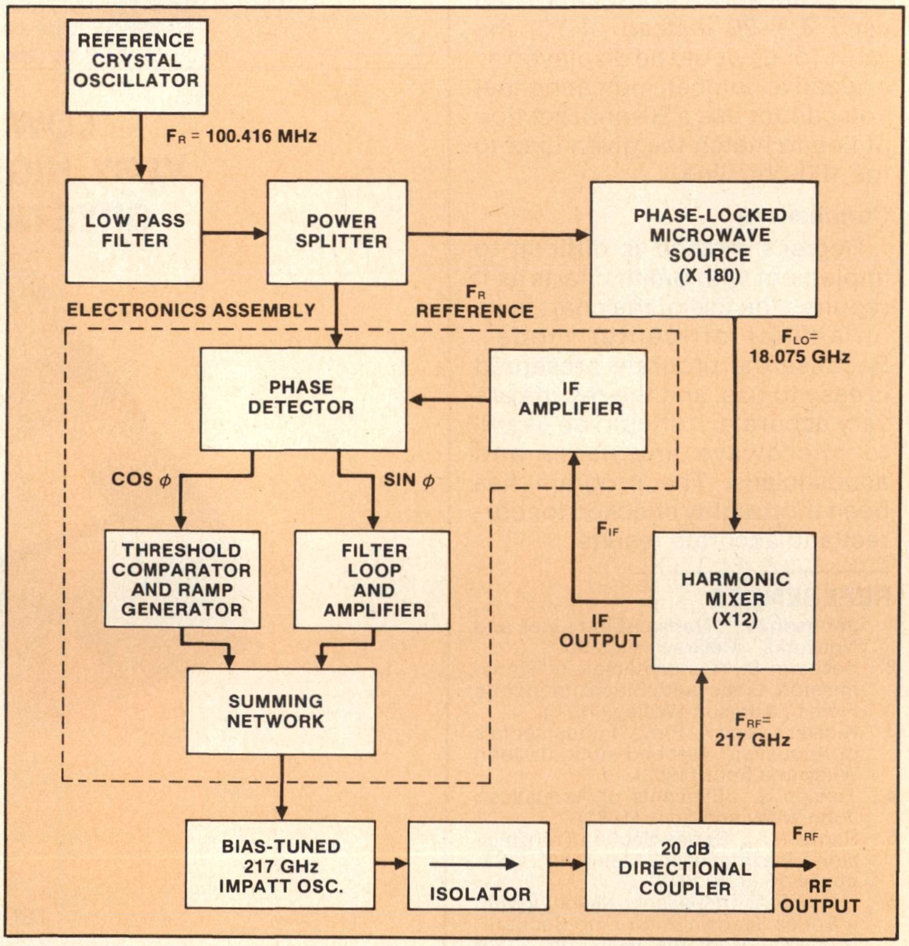

Fig. 1. Block diagram of 217 GHz phase-locked IMPATT oscillator.

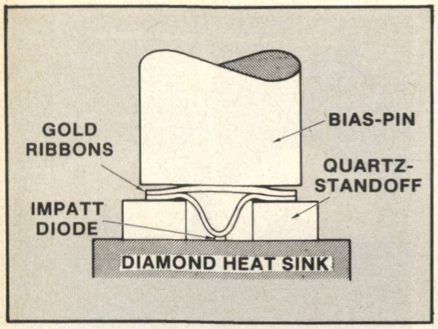

Fig. 2. Diode package

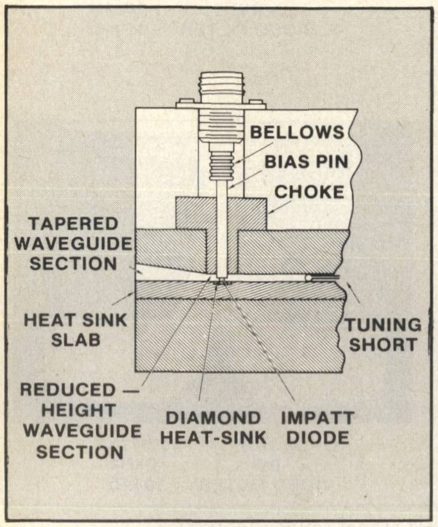

Fig. 3. Cross section of reduced height G-band oscillator circuit.

source. The frequency of the reference oscillator and the multiplying factor of the phase-locked micro-wave source are chosen so that when mixed with the desired millimeter-wave frequency F_{RF} they will produce an IF equal to that of the reference oscillator. A deviation of the millimeter-wave frequency due to frequency drift or phase noise will result in a shift in IF frequency away from the reference. Any difference in phase angle beteen F_R and F_{IF} can be detected by a phase detector and its outputs used as feedback to adjust the bias of the millimeter-wave source to eliminate this difference, thus phase-locking the millimeter-wave IMPATT oscillator.

IMPATT Source

The critical component in the system is the IMPATT millimeter-wave source. The source must provide the desired RF output power, frequency, and tuning sensitivity in the desired operating frequency range. The 217-GHz CW source utilizes a double-drift region silicon IMPATT diode.[3] The diode package is an open-type package design to minimize the parasitic inductance and capacitance as shown in Figure 2. The package consists of two quartz-standoffs with one ribbon contacting the diode and both quartz-standoffs. The second ribbon bridges the two quartz standoffs with the bias pin contacting this ribbon; it in effect parallels the diode-contacting ribbons and reduces the parasitic inductance. The bridge also mechanically strengthens the package assembly.

The diode is thermocompression bonded onto the diamond heatsink which is pressed into an OFHC copper slab. Since type IIA diamond provides a lower thermal impedance than copper, greater output with high reliability can be achieved with the diode on diamond heatsink.

The oscillator circuit is shown in Figure 3. The major sections are the tapered waveguide section which transforms from full G-band height to reduced height waveguide the reduced height waveguide section which contains the diode, and the mechanical tuning short section. The reduced height section improves the matching of the device impedance. The other pertinent components are the bias pin and the RF choke.

Table I shows the RF performance data of the CW source. As indicated, the output power is about 15 mW; taking into account the insertion losses of the isolator and the crossguide coupler, the output power of the phase-locked

[Continued on page 108]

TABLE I
RF Performance Data

Bias Conditions I_R(mA)	Bias Conditions V_R(V)	Frequency (GHz)	Output Power (mW)	Efficiency %
335	9.75	217.0	15	0.5

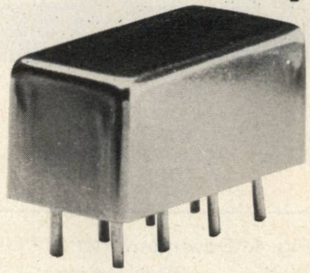

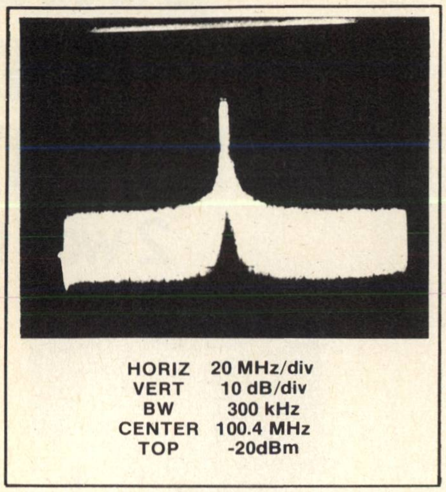

Fig. 4. Downconverter 217 GHz signal (free-running).

source is reduced to 5 mW.

The mechanical tunability of the IMPATT oscillator is approximately 6 GHz (212 GHz to 218 GHz) with the bias current held constant. The electrical tunability is approximately 3 GHz (215 GHz to 218 GHz) with the tuning short in a fixed position. In both cases, the output power was within 1.0 dB of the maximum output. The electrical tuning sensitivity is 15 MHz/mA

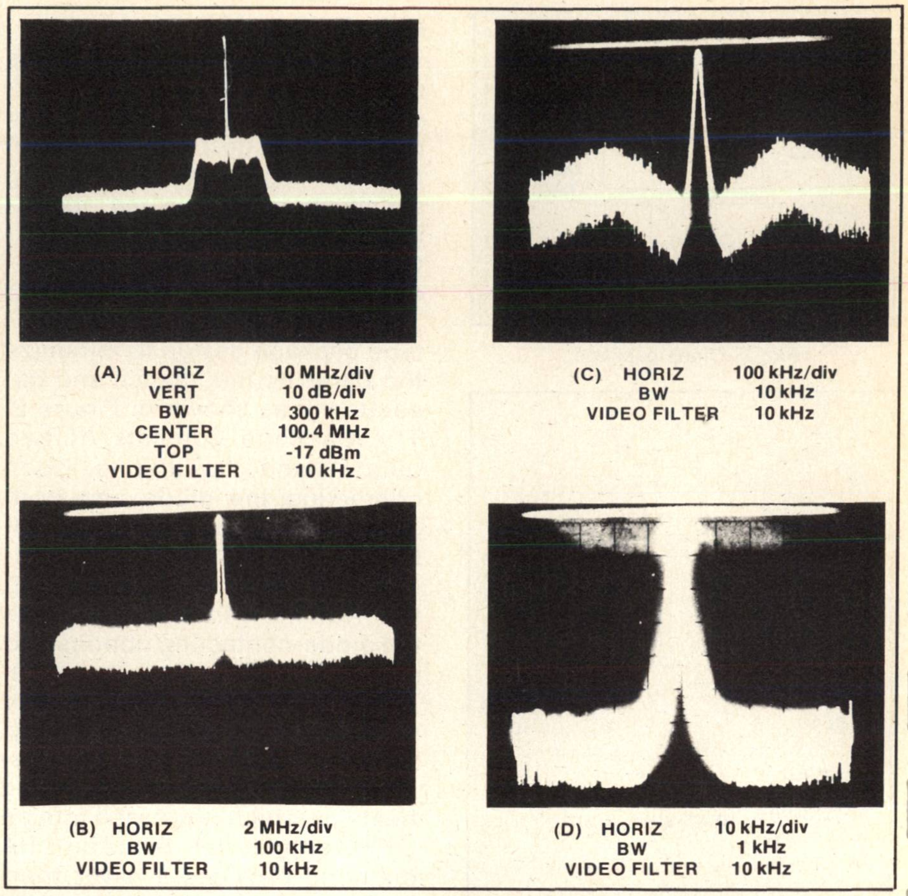

Fig. 5. Downconverter 217 GHz signal (phase-locked).

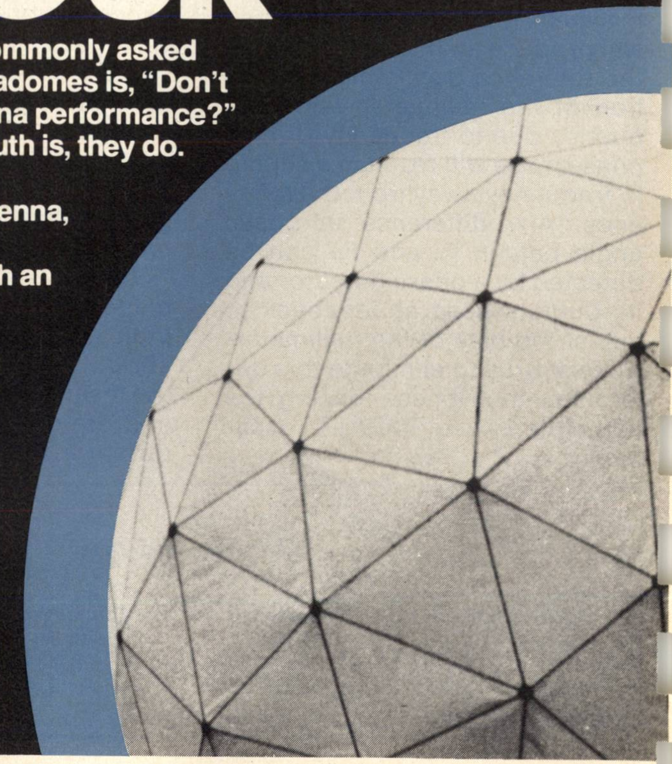

with the tuning short near the diode. The sensitivity decreases as the tuning short is moved away from the diode.

Detailed System Description

Referring to the system block diagram, Figure 1, the output of the reference crystal oscillator F_R is split two ways: one output is applied directly to the phase detector in the electronics assembly to serve as the phase reference; the second is applied to the phase-locked transistor microwave oscillator. The transistor oscillator source is itself a phase-locked system whose output frequency is 180 times the crystal frequency.

The output of the phase-locked oscillator F_{PLO} is used as the LO in the harmonic mixes. The sampled millimeter-wave oscillator signal near the desired operating frequency F_{RF} is then applied to the harmonic mixer and mixed with the twelfth harmonic of the local oscillator signal. The phase lock electronics compares the IF output signal of the harmonic mixer, F_{IF}, with the crystal frequency, F_R, and electrically tunes the IMPATT oscillator until F_{IF} becomes identical to F_R to lock at 217 GHz with the multiplication factors selected, the required crystal frequency is 100.41647 MHz.

System Performance

Figure 4 shows the free-running 217-GHz IMPATT source downconverted to 100 MHz as seen at the IF output of the harmonic mixer. The unlocked signal bandwidth of about 2 MHz (10 dB points) represents a total frequency jitter of about 1 part in 10^{-5}, (a remarkably small amount), most of which is due to power supply ripple. Such small values of free-running FM noise makes phase-locking possible with loop bandwidths smaller than 10 MHz. Figure 5A shows the downconverted phase-locked 217-GHz signal. Notice the reduction of FM noise content. Figures 5B, C, and D show the spectrum of the locked signal with increasing resolution.

Conclusion

The feasibility of phase-locking on IMPATT source in the 220-GHz region has been demonstrated. The applications of this technology include those requiring extreme frequency accuracy and stability (equal to percentage to that of the systems reference crystal oscillator). For example, frequency calibration, receiver local-oscillator source, injection-locking for high-powered CW and pulsed IMPATT sources and stable master oscillators for coherent radars.

Acknowledgements

The work was supported in part by the U.S. Army, BRL with Mr. R. McGee as Program Monitor. The authors also wish to extend their sincere appreciation to H. I. Ribet for his skilled laboratory assistance for the development of the phase-locked oscillator.

REFERENCES

1. Chang, K., F. Thrower, and G. Hayashibara, "Millimeter-Wave Si IMPATT Sources and Combiners", Presented at the 1981 IEEE MTT-S International Microwave Symposium
2. Cadwallader, J., and D. L. English, "Millimeter Front End Provide Frequency Agility", MSN, Vol 10, pp 41-53, December, 1980 ■